Published for SISSA by Springer

Received: April 7, 2014
Accepted: May 30, 2014
Published: June 18, 2014

Measurement of the low-mass Drell-Yan differential cross section at $\sqrt{s} = 7$ TeV using the ATLAS detector

The ATLAS collaboration

E-mail: atlas.publications@cern.ch

Abstract: The differential cross section for the process $Z/\gamma^* \to \ell\ell$ ($\ell = e, \mu$) as a function of dilepton invariant mass is measured in pp collisions at $\sqrt{s} = 7$ TeV at the LHC using the ATLAS detector. The measurement is performed in the e and μ channels for invariant masses between 26 GeV and 66 GeV using an integrated luminosity of 1.6 fb^{-1} collected in 2011 and these measurements are combined. The analysis is extended to invariant masses as low as 12 GeV in the muon channel using 35 pb^{-1} of data collected in 2010. The cross sections are determined within fiducial acceptance regions and corrections to extrapolate the measurements to the full kinematic range are provided. Next-to-next-to-leading-order QCD predictions provide a significantly better description of the results than next-to-leading-order QCD calculations, unless the latter are matched to a parton shower calculation.

Keywords: Hadron-Hadron Scattering

ArXiv ePrint: 1404.1212

doi:10.1007/JHEP06(2014)112

JHEP06(2014)112

Contents

JHEP06(2014)112

1 Introduction

The Drell-Yan (DY) process of dilepton production in hadronic interactions [1] provides important information on the partonic structure of hadrons which is distinct from that obtained in deep inelastic scattering (DIS) measurements (for a recent review see ref. [2] and the references therein). Recent measurements from ATLAS [3, 4], CMS [5–7] and LHCb [8, 9] provide further information in a new kinematic domain. Measurements reported here are made below the mass of the Z resonance and extend to a lower invariant mass than previous ATLAS measurements. In addition the cross sections are normalized by luminosity rather than to the Z mass peak cross section. The data are compared to theoretical calculations of the DY process, which can now reliably be performed at next-to-next-to-leading-order (NNLO) precision [10–13]. Calculations at next-to-leading-order (NLO) accuracy are also available matched to resummations at leading-logarithm (LL) or next-to-leading logarithm (NLL) precision [14, 15] to accommodate soft collinear partonic emission in the initial state. A quantitative comparison of the data to the calculations is presented including a QCD fit to the parton distribution functions, and a detailed discussion of theoretical uncertainties is given.

Measurements in the region of low dilepton invariant mass, $m_{\ell\ell} < 66\,\text{GeV}$, provide complementary constraints on the parton distribution functions (PDFs) to measurements near to the mass of the Z resonance. At low $m_{\ell\ell}$, the cross section is dominated by the electromagnetic coupling of $q\bar{q}$ pairs to the virtual photon (γ^*), whereas at masses near the Z pole the axial and vector weak couplings of the $q\bar{q}$ pair to the Z boson dominate. Therefore the observations reported here have a different sensitivity to up-type and down-type quarks and anti-quarks compared to measurements near the Z resonance.

The new kinematic region accessible at the LHC operating at a centre-of-mass energy of $\sqrt{s} = 7\,\text{TeV}$ and the rapidity coverage of the ATLAS detector allow low partonic momentum fractions, $x \sim 3 \times 10^{-4}$ to $\sim 1.7 \times 10^{-3}$, to be accessed at four-momentum transfer scales, Q, from $Q = m_{\ell\ell} \simeq 10\,\text{GeV}$ to 66 GeV. The values of x and Q probed are complementary to those reached at HERA [16].

The differential cross sections, $\mathrm{d}\sigma/\mathrm{d}m_{\ell\ell}$, are determined within two fiducial regions of acceptance in the electron and muon decay channels. The first measurement, termed the *nominal* analysis, is conducted in the region $26 < m_{\ell\ell} < 66\,\text{GeV}$. The minimum muon transverse momentum requirement, p_{T}^{μ}, and minimum electron transverse energy requirement, E_{T}^{e}, are 12 GeV. This analysis uses $1.6\,\text{fb}^{-1}$ of data collected in 2011, taking advantage of low-threshold triggers available in the first part of the 2011 data taking. This provides a statistical uncertainty on the measurement of less than 1%. A second measurement performed in the muon channel only, termed the *extended* analysis, is performed in a wider kinematic region spanning $12 < m_{\ell\ell} < 66\,\text{GeV}$. The minimum muon transverse momentum is reduced to 6 GeV by taking advantage of the lower trigger thresholds available from an integrated luminosity of $35\,\text{pb}^{-1}$ collected in 2010. Acceptance corrections are determined which allow the measurements to be extrapolated to the full phase space, where no kinematic cuts are applied. The fiducial measurements are compared to fixed-order perturbative quantum chromodynamic (QCD) calculations at NLO and NNLO, and NLO calculations matched to LL parton showers using PDFs from the MSTW [17] collaboration. In order to assess whether the measured cross sections can be well described with modified PDFs, a QCD fit is performed including HERA ep deep inelastic scattering data [16].

The ATLAS detector and the data and simulation samples are described in section 2 as are the triggers used in the analysis. The measurement selections, procedure and uncertainties are discussed in section 3. The cross-section measurements are presented in section 4 and are compared to the theoretical predictions and QCD fits. Finally, the results are summarised in section 5.

2 Data and simulation

2.1 ATLAS detector

The ATLAS detector [18] is a multi-purpose particle physics detector with forward-backward symmetric cylindrical geometry.[1] The inner detector (ID) system is immersed in

[1] ATLAS uses a right-handed coordinate system with its origin at the nominal interaction point (IP) in the centre of the detector and the z-axis along the beam pipe. The x-axis points from the IP to the centre of the LHC ring, and the y-axis points upward. Cylindrical coordinates (r, ϕ) are used in the transverse plane, ϕ being the azimuthal angle around the beam pipe. The pseudorapidity is defined in terms of the polar angle θ as $\eta = -\ln\tan(\theta/2)$.

JHEP06(2014)112

a 2 T axial magnetic field and measures the trajectories of charged particles in the pseudorapidity range $|\eta| < 2.5$. It consists of a semiconductor pixel detector, a silicon microstrip detector, and a transition radiation tracker, which is also used for electron identification.

The calorimeter system covers the pseudorapidity range $|\eta| < 4.9$. The highly segmented electromagnetic calorimeter consists of lead absorbers with liquid argon (LAr) as active material and covers the pseudorapidity range $|\eta| < 3.2$. In the region $|\eta| < 1.8$, a presampler detector using a thin layer of LAr is used to correct for the energy lost by electrons and photons upstream of the calorimeter. The barrel hadronic calorimeter is a steel and scintillator-tile detector and is situated directly outside the envelope of the barrel electromagnetic calorimeter. It covers a pseudorapidity range $|\eta| < 1.7$. The two endcap hadronic calorimeters have LAr as the active material and copper absorbers and cover a pseudorapidity range of $1.5 < |\eta| < 3.2$. The forward calorimeter provides coverage of $3.1 < |\eta| < 4.9$ using LAr as the active material and copper and tungsten as the absorber material.

The muon spectrometer (MS) measures the trajectory of muons in the large superconducting air-core toroid magnets. It covers the pseudorapidity range $|\eta| < 2.7$ and is instrumented with separate trigger and high-precision tracking chambers arranged in three layers with increasing distance from the interaction point. A precision measurement of the track coordinates in the principal bending direction of the magnetic field is provided by drift tubes in all three layers within the pseudorapidity range $|\eta| < 2.0$. At large pseudorapidities, cathode strip chambers with higher granularity are used in the innermost plane over $2.0 < |\eta| < 2.7$. The muon trigger system, which covers the pseudorapidity range $|\eta| < 2.4$, consists of resistive plate chambers in the barrel ($|\eta| < 1.05$) and thin gap chambers in the endcap regions ($1.05 < |\eta| < 2.4$).

A three-level trigger system is used to select events for offline analysis. The level-1 trigger is implemented in hardware and uses a subset of detector information to reduce the event rate to a design value of at most 75 kHz. This is followed by two software-based trigger levels, level-2 and the event filter, which together reduce the event rate to a few hundred Hz which is recorded for offline analysis.

2.2 Event triggering

Events are recorded by dilepton (electron or muon) triggers using different trigger configurations to obtain the data in 2010 and 2011.

The 2010 data were selected by a low-threshold di-muon trigger with a transverse momentum trigger threshold of 4 GeV. The muons are required to have opposite charge, originate from the same event vertex, and satisfy $m_{\ell\ell} > 0.5\,\text{GeV}$. The muon trigger efficiency is determined from a large sample of $J/\psi \to \mu\mu$ events and is measured differentially in the transverse momentum p_{T}^{μ} and pseudorapidity of the muon, η^{μ}. Due to significant charge dependence at low p_{T}^{μ} and high pseudorapidity, separate trigger efficiencies are produced for positive and negative muons. From these results, the efficiency of the di-muon trigger conditions are obtained differentially in $m_{\ell\ell}$.

The 2011 muon data were collected with a di-muon trigger with a transverse momentum threshold of 10 GeV. The efficiency was determined using a tag-and-probe method

JHEP06(2014)112

on a $Z \to \mu\mu$ sample recorded using a single-muon trigger with an 18 GeV transverse momentum threshold.

The di-electron trigger uses calorimetric information to identify two narrow electromagnetic energy depositions. Electron identification algorithms use further calorimetric information on the shower shape and fast track reconstruction to find electron candidates with a minimum required transverse energy of 12 GeV. The efficiency as a function of transverse energy and pseudorapidity of the electron is determined using a $Z \to ee$ sample recorded using a single-electron trigger with a 20 GeV E_{T} threshold, following ref. [19].

2.3 Simulation

Drell-Yan signal events are simulated using Pythia 6.426 [20] together with leading-order MRST LO* [21] parton distribution functions. Higher-order effects are approximated by the application of NNLO K-factors computed with the Vrap 0.9 program [22]. Pythia 6.426 is also used to simulate $Z/\gamma^* \to \tau\tau$, $W \to \mu\nu$ and $W \to e\nu$ processes, which are scaled using NNLO K-factors.

The Mc@nlo 3.42 [14] generator is used to simulate $t\bar{t}$ production and is also scaled to NNLO accuracy using a K-factor [23–28]. Diboson (WW, WZ, ZZ) production is simulated using the Herwig 6.520 [29] generator in conjunction with K-factors computed at NLO precision. Since the multijet background is difficult to simulate accurately, it is estimated using data-driven techniques supplemented with Pythia 6.426 simulation of heavy-flavour ($b\bar{b}, c\bar{c}$) jet production.

The Monte Carlo (MC) generators are interfaced to Tauola 2.4 [30] and Photos 3.0 [31] to describe τ decays and the effects of QED final-state radiation respectively. Multiple pp collisions within a single bunch crossing, referred to as pile-up interactions, are accounted for by overlaying simulated minimum-bias events produced in Pythia tuned to ATLAS data [32, 33].

The generated particle four-momenta are passed through the ATLAS detector simulation [34], which is based on Geant4 [35]. The simulated events are reconstructed and selected using the same software chain as for data. The MC samples are adjusted using factors derived from data to reflect mismodellings of the lepton momentum scale and resolution, trigger efficiency, lepton reconstruction efficiency, and isolation efficiencies [19, 36–38]. No corrections are applied to the MC simulation to improve the description of the dilepton p_{T} spectrum; however the influence of this effect is assessed in section 3.5.

Theoretical predictions of the fiducial cross sections were computed for comparison to the measured cross sections. Fewz 3.1b2 [13, 39–41] provides a full NLO and NNLO calculation with higher-order electroweak (HOEW) corrections included. To avoid double-counting with the QED final-state radiation effects simulated with Photos, the HOEW corrections calculated by Fewz are chosen to exclude this effect. The HOEW calculation uses the G_μ electroweak parameter scheme [42], in which large higher-order corrections are already absorbed in the precisely measured muon decay constant G_μ. This is used as input to the electroweak calculations together with M_W and M_Z, the W and Z boson masses respectively [43]. The renormalisation and factorisation scales are set to $\mu_R = \mu_F =$

JHEP06(2014)112

$m_{\ell\ell}$. The HOEW corrections are verified by comparisons with calculations performed with SANC [44, 45].

The fiducial cross section is also compared to POWHEG [15, 46–48], which provides an NLO prediction with a leading-log parton shower (LLPS) matched to the matrix element calculation. It is also performed in the G_μ electroweak scheme, with scales $\mu_R = \mu_F = m_{\ell\ell}$. These theoretical predictions are supplemented with HOEW corrections which are calculated separately in FEWZ at NLO in QCD.

3 Experimental procedure

Events are required to be taken during stable beam condition periods and must pass detector and data-quality requirements. At least one vertex from a proton-proton collision, referred to a as a primary vertex, reconstructed from at least three tracks is required in each event. Leptons produced in the Drell-Yan process are expected to be well isolated from any energy associated with jets. The degree of isolation for electrons is defined as the scalar sum of transverse energy, $\sum E_{\mathrm{T}}$, of additional particles contained in a cone of size $\Delta R = \sqrt{(\Delta\phi)^2 + (\Delta\eta)^2}$ around the electron, divided by E^e_{T}, the transverse energy of the electron. For muons the isolation is defined using the scalar sum of transverse momentum, $\sum p_{\mathrm{T}}$, of additional tracks divided by p^μ_{T}, the transverse momentum of the muon. These two measures of isolation provide a good discriminant against backgrounds arising from multijet production, where the dominant contribution is from semileptonic decays of heavy quarks. The electron and muon channels utilise different methods to estimate the multijet background due to the differences between calorimetric and track based isolation criteria, and are discussed in detail below. The contributions from multijet processes and from $Z/\gamma^* \to \tau\tau$ decays are the two most significant backgrounds to the signal. Additional backgrounds can arise from events in which a jet fakes a lepton in association with a real lepton, for example in W+jet production. Smaller background contributions are seen from $t\bar{t}$ and diboson ($WW/WZ/ZZ$) leptonic decays in both the nominal and extended analyses.

Asymmetric minimum lepton E_{T} or p_{T} requirements are used in the event selections to avoid the kinematic region of $2p_{\mathrm{T}} \sim m_{\ell\ell}$ where perturbative QCD calculations are unstable and can lead to unphysical predictions [49].

Due to the different kinematic ranges and detector response to electrons and muons, the selection is optimised separately for each channel and is described in the following.

3.1 Electron channel

Electrons are reconstructed using a sliding-window algorithm which matches clusters of energy deposited in the electromagnetic calorimeter to tracks reconstructed in the inner detector. The calorimeter provides the energy measurement and the track is used to determine the angular information of the electron trajectory. Candidates are required to be well within the tracking region, $|\eta^e| < 2.4$ of the inner detector excluding a region, $1.37 < |\eta^e| < 1.52$, where the transition between the barrel and endcap electromagnetic calorimeters is difficult to model with the simulation. Each candidate is required to satisfy

JHEP06(2014)112

tight electron identification [19] criteria. In order to further increase the purity, calorimetric isolation is used, with $\sum E_{\mathrm{T}}/E_{\mathrm{T}}^{e}$ requirements within a cone of $\Delta R = 0.4$ applied as a function of η_e. The maximum isolation value is adjusted to maintain a constant estimated signal efficiency of approximately 98%.

Candidate DY events are required to have exactly two oppositely charged electrons with $E_{\mathrm{T}}^{e} > 12\,\mathrm{GeV}$ and at least one of the electrons satisfying $E_{\mathrm{T}}^{e} > 15\,\mathrm{GeV}$. The invariant mass of the pair is required to be between $26 < m_{ee} < 66\,\mathrm{GeV}$. The selection efficiencies from the electron reconstruction, identification, calorimeter isolation and trigger requirements are determined from $Z \to ee$, $W \to e\nu$ and $J/\psi \to ee$ event samples in bins of η^{e} and E_{T}^{e} using a tag-and-probe method [19]. The MC simulation is then corrected to reproduce the efficiencies in the data.

Inclusive multijet production is the largest source of background and gives rise to fake electron signatures, as well as real electrons from the semileptonic decays of b and c heavy quarks (HQ). The background contribution from $W \to e\nu$ also gives rise to real and fake electron signatures. Fake electrons are produced in equal number for positive and negative charges, therefore this background can be estimated from the number of same-sign (SS) electron pairs in the data and is subtracted from the opposite-sign (OS) electron pair sample. The number of events with electrons from HQ decays are reduced by a factor of three by the isolation requirement.

After subtracting the SS contribution and the background from $Z/\gamma^{*} \to \tau\tau$, $t\bar{t}$ and diboson processes using MC predictions, the remaining HQ contribution is estimated from data. In these background processes the lepton isolation distribution is expected to be the same for ee and $e\mu$ pairs. Therefore the HQ contribution in the signal region can be estimated under the assumption that the ratio of the number of ee to $e\mu$ pairs in which both leptons fail the isolation requirement is the same as the ratio of the number of ee to $e\mu$ pairs in which both leptons pass the isolation requirement. In this estimation procedure the muon isolation is defined by replacing $\sum p_{\mathrm{T}}$ with $\sum E_{\mathrm{T}}$ in order to ensure similar behaviour between ee and $e\mu$ pairs. The signal contamination of the non-isolated ee sample is about 1% and is subtracted using the MC simulation. The $e\mu$ pairs are selected from a sample of data triggered by a muon with at least $p_{\mathrm{T}}^{\mu} > 6\,\mathrm{GeV}$ and an electron with $E_{\mathrm{T}}^{e} > 10\,\mathrm{GeV}$. Leptons identified in this sample were required to have $E_{\mathrm{T}}^{\ell} > 12\,\mathrm{GeV}$ and were subject to the same E_{T}, η and isolation criteria for selection as the ee pairs.

The background from HQ processes decreases from 15% at the lowest $m_{\ell\ell}$ to 5% at the highest $m_{\ell\ell}$. The SS estimate of fake electron pairs from jets ranges between 5% and 3%. As a cross check the $W \to e\nu$ background estimated from simulation is found to be 0.2% of all selected events in data. The $Z/\gamma^{*} \to \tau\tau$ process contribution reaches a maximum of 7% at $m_{\ell\ell} \sim 50\,\mathrm{GeV}$ falling to 1% at low invariant mass. The $t\bar{t}$ and diboson leptonic decays contribute 1% and 0.2% of the total number of observed electron pairs, respectively.

The invariant mass distribution, m_{ee}, of the final selected sample of data is shown in figure 1, and is compared to simulations of signal and all significant background processes. The agreement between the data and the expected signal plus estimated background is good.

JHEP06(2014)112

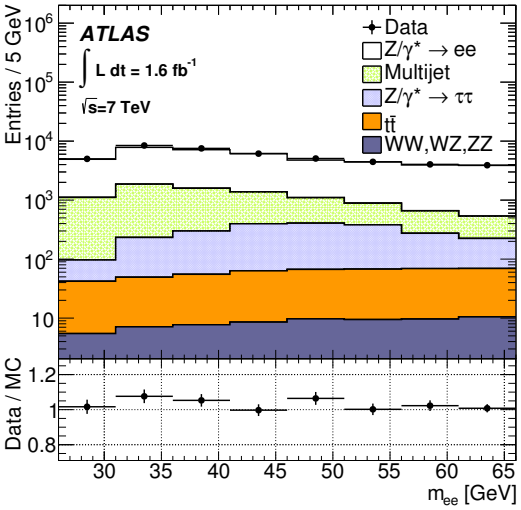

Figure 1. Distribution of di-electron invariant mass m_{ee} for the nominal analysis selection. The error bars for the ratio represent statistical uncertainties of the data and Monte Carlo samples.

3.2 Muon channel

Events in the nominal muon-channel analysis are selected online by a trigger requiring two muon candidates with $p_{\mathrm{T}}^{\mu} > 10\,\mathrm{GeV}$. Muons are identified by tracks reconstructed in the muon spectrometer matched to tracks reconstructed in the inner detector, and are required to have $p_{\mathrm{T}}^{\mu} > 12\,\mathrm{GeV}$ and $|\eta^{\mu}| < 2.4$. In addition, one muon is required to have $p_{\mathrm{T}}^{\mu} > 15\,\mathrm{GeV}$. Isolated muons are selected by requiring $\sum p_{\mathrm{T}}/p_{\mathrm{T}}^{\mu} < 0.18$ within a cone of $\Delta R = 0.4$. The two highest p_{T}^{μ} muons should have opposite charge, and no veto on additional muons is applied. Finally, candidate events are required to have $26 < m_{\ell\ell} < 66\,\mathrm{GeV}$. The muon track reconstruction efficiency, trigger efficiency, isolation cut efficiency, as well as the muon momentum scale and resolution [38] are measured and calibrated using a tag-and-probe method with $Z \to \mu\mu$ and $J/\psi \to \mu\mu$ event samples. The MC simulation is adjusted to describe the data for each of the above effects. The trigger efficiency corrections are parameterised as a function of η^{μ}, p_{T}^{μ} and muon charge; the muon reconstruction efficiency corrections [36] are determined as a function of η^{μ}, p_{T}^{μ} and ϕ^{μ}; and the muon isolation efficiency corrections are determined as a function of p_{T}^{μ} only.

The main backgrounds arise from $Z/\gamma^* \to \tau\tau$ where the τ leptons decay leptonically to muons, and from multijet production in which c- and b- quark mesons decay to muons. To estimate the size of the multijet background contribution, a partially data-driven two-component template fit is employed. The multijet background is modelled using a MC sample of heavy-flavour $b\bar{b}$ and $c\bar{c}$ jets, and a background sample obtained from SS muon pairs taken from data. The SS data sample accounts for any light-flavour jets and mis-modelling of the isolation spectrum.

A pure multijet background sample is obtained by requiring all selection cuts except the isolation cut, which is replaced by a stringent anti-isolation requirement $\sum p_{\mathrm{T}}/p_{\mathrm{T}}^{\mu} > 0.38$ placed on one muon in the pair. The muon is chosen at random to avoid correlations in p_{T}^{μ},

JHEP06(2014)112

η^μ and charge. The second muon then provides the shape of the multijet isolation spectrum. Templates are constructed from the SS muon pairs in data and heavy-flavour MC simulation, which has the MC simulation SS muon pairs subtracted to avoid double counting, using the same anti-isolation requirement. The templates are then fitted to the OS multijet isolation spectrum to obtain the normalisation of each component. The procedure is validated by comparing the isolation spectrum for data with the sum of all background contributions after applying all selections except the isolation cut. This method provides a significantly better description of the isolation spectrum than MC simulation alone.

After the complete selection and application of the normalisation of the two multijet components, the total multijet background is found to constitute 5% of the selected data sample at low $m_{\ell\ell}$ decreasing to 1% at the highest $m_{\ell\ell}$, and the $Z/\gamma^* \to \tau\tau$ contribution ranges between 1% and 6% respectively. All remaining backgrounds together contribute less than 1% of the selected number of data events.

Figure 2 shows the distribution of invariant mass $m_{\mu\mu}$ in data after all selections are applied. A comparison to the simulated signal sample and all significant backgrounds is shown. Within statistical uncertaities, a good description of the data is achieved.

3.3 Low-mass extended analysis

For the low-mass extended analysis, reconstructed muons are required to have $p_{\mathrm{T}}^{\mu} > 6\,\mathrm{GeV}$ and $|\eta^{\mu}| < 2.4$. In addition, one muon is required to have $p_{\mathrm{T}}^{\mu} > 9\,\mathrm{GeV}$. Since the multijet background is larger at lower values of p_{T}^{μ}, stringent background suppression is employed by requiring the muon isolation to be $\sum p_{\mathrm{T}}/p_{\mathrm{T}}^{\mu} < 0.08$ within a cone of $\Delta R = 0.6$. This criterion is estimated from MC simulation to have a signal efficiency of 73% and a background rejection of 96%. The reduced p_{T}^{μ} requirement compared to the nominal analysis allows the measurement to be extended to lower invariant masses. Events are required to have $12 < m_{\ell\ell} < 66\,\mathrm{GeV}$.

As for the nominal muon analysis, the trigger and muon track reconstruction efficiency, isolation cut efficiency, the muon momentum scale and resolution are all determined using large samples of Z and J/ψ decaying to $\mu\mu$. The MC simulation is adjusted to better describe the data as detailed elsewhere [36, 38, 50].

The largest background source comes from multijet production, which corresponds to 23% of the selected data sample at low $m_{\ell\ell}$, falling to 6% at the highest $m_{\ell\ell}$, and depends strongly on the muon isolation requirement. The multijet contribution is estimated using the same template fit method as for the nominal analysis with the only difference being the anti-isolation selection of $\sum p_{\mathrm{T}}/p_{\mathrm{T}}^{\mu} > 1.0$ on one muon. All other background contributions are at least a factor ten smaller and are estimated from the MC samples.

Figure 3 shows the distribution of invariant mass after all selection requirements for the data together with the expected contributions from all simulation samples for signal and background processes. Within statistical uncertainties, a good description is achieved.

3.4 Cross-section measurement

The differential cross section $\mathrm{d}\sigma/\mathrm{d}m_{\ell\ell}$ is determined by subtracting the estimated background from the observed number of events and unfolding the data for detector acceptance,

JHEP06(2014)112

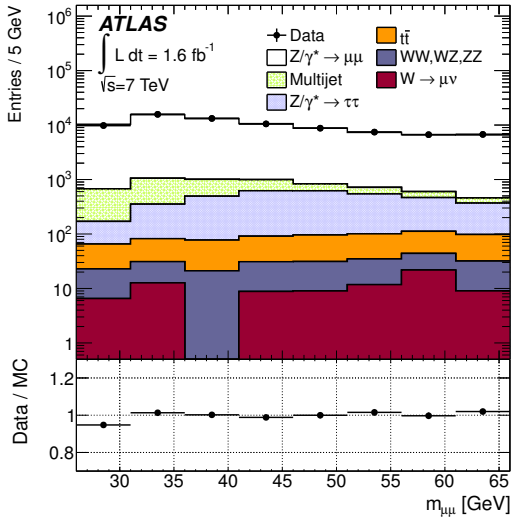

Figure 2. Distributions of the di-muon invariant mass $m_{\mu\mu}$ for the nominal analysis selection. The lower panel shows the ratio of the data and Monte Carlo samples. The statistical uncertainties included in the figure are too small to be visible.

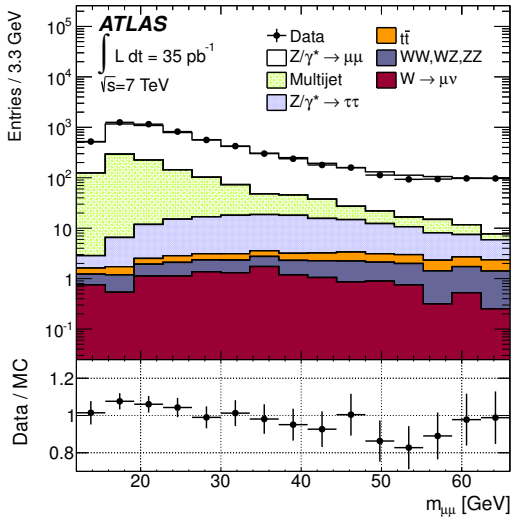

Figure 3. Distributions of the di-muon invariant mass $m_{\mu\mu}$ for the extended analysis selection. The error bars for the ratio represent statistical uncertainties of the data and Monte Carlo samples.

selection efficiency and resolution effects using the signal simulation samples. The unfolding also accounts for QED final-state radiation (FSR), and is referred to as unfolding to the Born level. The cross sections may also be obtained at the so-called "dressed" level with respect to QED FSR, in which the leptons are recombined with any final-state photon radiation from the leptons within a cone of $\Delta R = 0.1$ around each lepton.

The unfolded measurements are presented for a common fiducial acceptance in the electron and muon nominal analyses within a dilepton invariant mass of $26 < m_{\ell\ell} < 66$ GeV.

JHEP06(2014)112

The nominal fiducial acceptance is defined as $|\eta^\ell| < 2.4$, $p_{\mathrm{T}}^\ell > 15\,\mathrm{GeV}$ for the leading lepton and $p_{\mathrm{T}}^\ell > 12\,\mathrm{GeV}$ for the sub-leading lepton, where $\ell = e\,,\mu$. The fiducial region for the extended analysis is defined as $|\eta^\ell| < 2.4$, $p_{\mathrm{T}}^\ell > 9\,\mathrm{GeV}$ for the leading lepton and $p_{\mathrm{T}}^\ell > 6\,\mathrm{GeV}$ for the sub-leading lepton, and dilepton invariant mass of $12 < m_{\ell\ell} < 66\,\mathrm{GeV}$.

The muon-channel measurements are unfolded using a bin-by-bin correction procedure. The bin widths are chosen to ensure high purity, defined as the fraction of reconstructed signal events in a given bin of $m_{\mu\mu}$ which were also generated in the same bin. For the nominal analysis the bin purity is above 80% in all bins, and for the extended analysis it is always above 87% due to the larger bin widths suited to the lower integrated luminosity for this analysis.

The differential fiducial cross section for the process $pp \to Z/\gamma^* \to \mu\mu$ is determined in each measurement bin according to

$$\frac{\mathrm{d}\sigma}{\mathrm{d}m_{\ell\ell}} = \frac{N - B}{\mathcal{L}\,\mathcal{C}\,\Delta m_{\ell\ell}},$$

where N and B are the number of observed events and the estimated number of background events respectively, $\mathcal{C}$ is the overall signal selection efficiency and resolution smearing correction factor determined from MC simulation, $\mathcal{L}$ is the integrated luminosity of the data sample, and $\Delta m_{\ell\ell}$ is the bin width. The $\mathcal{C}$ factor is defined as the ratio of the number of reconstructed MC signal events passing the selection to the number of generated MC signal events satisfying the fiducial requirements in a given bin of $m_{\ell\ell}$ at the Born level. No bin centre corrections are applied for either the muon or electron analysis.

In the electron-channel analysis the unfolding is performed using an iterative Bayesian unfolding technique [51] due to a bin purity of 75% at low $m_{\ell\ell}$, which falls to 51% at the highest $m_{\ell\ell}$. The low purity at $m_{\ell\ell} \sim 60\,\mathrm{GeV}$ is due to a combination of intrinsic detector resolution, and migrations from the Z resonance peak region due to FSR as well as the energy loss of electrons in the material in front of the calorimeter. The differential fiducial cross section for the process $pp \to Z/\gamma^* \to ee$ is obtained using the relation

$$\frac{\mathrm{d}\sigma}{\mathrm{d}m_{\ell\ell}} = \frac{1}{\mathcal{L}\,\Delta m_{\ell\ell}}\mathcal{R}\frac{N - B}{\epsilon},$$

where ϵ includes the trigger, isolation and electron identification efficiencies, and $\mathcal{R}$ is the response matrix. This accounts for resolution smearing, reconstruction efficiency effects, acceptance corrections for the region $1.37 < |\eta^e| < 1.52$ and unfolds the observed efficiency-corrected distribution to the Born level.

For both the electron and muon channels, the correction from the measured kinematics to the Born-level kinematics is included in the $\mathcal{R}$ and $\mathcal{C}$ factors respectively and can be as large as $\sim 30\%$ for $m_{\ell\ell} \sim 60\,\mathrm{GeV}$ due to wide-angle QED FSR radiation causing migration of events from the Z resonance peak to lower $m_{\ell\ell}$. Very good agreement in the QED FSR predictions were found between Photos and Sanc [45]. The corrections to the dressed level, $\mathcal{D}$, are also obtained from MC samples, and are close to unity, but increase close to $m_{ll} \sim 60\,\mathrm{GeV}$ for the same reason since the $\Delta R = 0.1$ cone does not include all photons from wide-angle radiation.

JHEP06(2014)112

The fiducial cross sections may be corrected to the full kinematic range, with no lepton p_{T}^{ℓ} or η^{ℓ} restrictions, by applying an acceptance correction factor, $\mathcal{A}$, determined from FEWZ and calculated at NNLO. Correction factors from the Born to the dressed level, and from the fiducial to the full kinematic range are provided in the cross-section tables in section 4.

3.5 Systematic uncertainties

The systematic uncertainties on the measured cross sections are estimated by repeating the measurement after varying each source of uncertainty in the MC samples. The multijet background uncertainties are determined from the comparison of different estimation methods using data and MC simulation.

In the nominal electron channel, the detector resolution, energy scale, and reconstruction efficiency uncertainties are propagated to the measured cross sections by varying the MC simulation used to determine the response matrix $\mathcal{R}$. The data and MC statistical uncertainties are propagated by sets of pseudo-experiments where the measured spectrum and the response matrix elements are varied by their statistical uncertainties. The contribution to the uncertainty on the unfolded spectrum due to the data and MC sample size, referred to as the statistical uncertainty on the unfolding, is 1.8% in the lowest mass bin and 0.4% in the highest. Variations of the electron energy resolution and scale uncertainties yields a negligible effect. Varying the reconstruction efficiency in the MC simulation within its uncertainty yields correlated systematic uncertainties between mass bins ranging from 2.3% in the lowest mass bin to 0.3% in the highest. Statistical components of the systematic uncertainties are propagated to the cross-section measurements using an ensemble of pseudo-experiments in which replicas of the corrections are constructed by random variation within their statistical uncertainties.

The effects of the electron trigger, identification and isolation requirements on the DY-pair selection efficiency are evaluated using MC simulation by varying the correction factors that account for the mismodellings of these selection criteria in the MC simulation. The uncertainty on the electron identification efficiency is partially correlated between mass bins. The correlated component ranges from 1% in the lowest mass bin to 0.1% in the highest. The uncorrelated component is 1.2% in the lowest mass bin decreasing to 0.2% in the highest. The trigger and isolation efficiency uncertainties are treated as uncorrelated and are estimated by varying the selection criteria used to measure these efficiencies. The uncertainty varies from 0.1–0.6% and 0.2–1.4% due to the trigger and isolation efficiencies, respectively.

The multijet background uncertainty in the nominal electron channel is largely due to statistical uncertainties of the $e\mu$ pairs used in the method. Systematic uncertainties are evaluated by varying the non-isolation requirement, and the subtracted $Z/\gamma^{*} \to \tau\tau$ and $t\bar{t}$ contributions in the isolated $e\mu$ sideband region by their uncertainties. The total uncertainty on the multijet background is approximately 15%, which corresponds to a fiducial cross-section measurement uncertainty of 3.9% in the lowest mass bin and 1.6% in the highest. The contributions from the electroweak ($Z/\gamma^{*} \to \tau\tau$, $t\bar{t}$ and diboson) backgrounds are estimated using simulation with an uncertainty of 5% on the production

JHEP06(2014)112

cross sections of $Z/\gamma^* \to \tau\tau$ and diboson, and 6% on the production cross section of $t\bar{t}$, corresponding to an uncertainty between 0.3% and 1.0% on the measured cross sections.

An uncertainty of typically less than 1% is assigned to the cross section due to the effect of reweighting the di-electron p_{T} spectrum to the spectrum of a different model which describes the ATLAS measurement at the Z resonance better [52]. An uncertainty of 1.2% accounts for the uncertainty in the GEANT4 detector simulation due to mismodelling of electron multiple scattering.

The efficiency of the muon reconstruction algorithms is well modelled in the simulation. The uncertainty is partially correlated between mass bins. The correlated part has a residual uncertainty of better than 0.3% over the full η^μ and p_{T}^μ range in the nominal analysis. For the extended analysis the uncertainty is similar to the nominal analysis for $p_{\mathrm{T}}^\mu > 10\,\mathrm{GeV}$, but increases to 1.1–1.7% at lower p_{T}^μ.

The muon momentum calibration and resolution uncertainties typically contribute 0.5% or less to the measurements in both muon-channel analyses. The muon trigger efficiency uncertainty in the nominal analysis is estimated by varying the $Z \to \mu\mu$ control sample selection criteria. At low p_{T}^ℓ the statistical component of the uncertainty increases and is propagated to the cross-section measurement using the pseudo-experiment method. In the extended analysis the uncertainty is dominated by the variation of the background contribution in the J/ψ resonance sample, and the statistical sample size used to estimate the efficiency.

For the nominal muon analysis the isolation efficiency uncertainty arises from variations of the selection criteria used to determine the efficiency and is estimated to be 2% for $p_{\mathrm{T}}^\mu < 16\,\mathrm{GeV}$, better than 0.5% elsewhere. In the extended analysis this uncertainty arises from the variation of the subtracted multijet background and the difference between two control samples used to estimate the uncertainty.

The $Z/\gamma^* \to \tau\tau$, diboson, W production, and $t\bar{t}$ production backgrounds for both muon-channel analyses are estimated using simulation with an uncertainty of 5% on the production cross sections, except for $t\bar{t}$ production where the uncertainty is taken to be 6%.

The multijet background uncertainty is estimated by comparing the data and simulation in the isolation spectrum, and by comparing $m_{\ell\ell}$ distributions for data and simulation with an inverted isolation requirement. For the nominal analysis the agreement in both spectra is better than 20% whereas for the extended analysis the agreement is better than 10%. Variations of the background by these amounts lead to cross-section uncertainties of 0.3–1.1% for the nominal measurements, and 0.7–3.0% for the extended measurements where the multijet background contribution is substantially larger. As with the electron channel, an uncertainty is applied to the nominal muon cross section from the reweighting of the di-muon p_{T} spectra, and this is seen to be $< 0.3\%$.

The uncertainty in the luminosity measurement of the ATLAS detector is fully correlated point-to-point and also correlated between the nominal electron and muon channel measurements. It is 1.8% for the nominal analysis and 3.5% for the extended analysis [53]. All systematic uncertainties, including the uncertainty on the luminosity measurement, are uncorrelated between the extended and nominal analyses.

JHEP06(2014)112

m_{ee}	$\frac{d\sigma}{dm_{ee}}$	δ^{stat}	δ^{syst}	δ^{total}
[GeV]	[pb/GeV]	[%]	[%]	[%]
26–31	2.02	1.4	6.0	6.1
31–36	3.41	1.1	5.2	5.3
36–41	2.81	1.2	4.6	4.7
41–46	1.97	1.3	4.6	4.8
46–51	1.62	1.4	4.1	4.3
51–56	1.25	1.5	3.8	4.1
56–61	1.02	1.6	3.4	3.7
61–66	0.91	1.6	2.8	3.2

Table 1. The nominal electron-channel differential Born-level fiducial cross section, $\frac{d\sigma}{dm_{ee}}$. The statistical, δ^{stat}, systematic, δ^{syst} and total, δ^{total}, uncertainties are given for each invariant m_{ee} mass bin. The luminosity uncertainty (1.8%) is not included.

4 Results

4.1 Nominal analysis

The measured Born-level fiducial cross sections for the nominal electron analysis are presented in table 1, and the complete evaluation of the individual systematic uncertainties is provided in table 2, excluding the normalisation uncertainty arising from the luminosity measurement. The sources are separated into those which are point-to-point correlated and uncorrelated. The precision of the electron-channel measurements is limited by the uncertainties associated with the multijet background estimation and the electron reconstruction efficiency.

The nominal muon-channel Born-level fiducial cross section measurements are presented in table 3. The breakdown of the systematic uncertainties for the correlated and uncorrelated sources is given in table 4. The precision of the measurements is limited by the isolation efficiency determination at low $m_{\mu\mu}$.

Measurements made in the nominal analysis are defined with a common fiducial acceptance and are in good agreement with each other. A combination of the nominal e and μ measurements is performed using a χ^2 minimisation technique taking into account the point-to-point correlated systematic uncertainties of the measurements and correlations between the electron and muon channels [16, 54, 55]. This method introduces a free nuisance parameter for each correlated systematic error source which contributes to the total χ^2 and therefore gives results that are different from a simple weighted average. The combination procedure yields a total χ^2 per degree of freedom (n_{dof}) of $\chi^2/n_{dof} = 6.4/8$. There is no experimental source of systematic uncertainty that is shifted by more than one standard deviation in the combination. The comparison of the measured and combined cross sections is shown in figure 4. The electron-channel measurements have a tendency to be larger than the muon-channel cross sections, although they are in agreement within their uncertainties. The combined measurements are given in table 5, which also includes the resulting correlated uncertainty contributions after the minimisation procedure. The total uncertainty of the cross-section measurements, excluding the luminosity uncertainty, is reduced to 1.6–3% across the measured range.

JHEP06(2014)112

	Correlated						Uncorrelated					
m_{ee}	$\delta^{\text{e.w.}}_{\text{cor}}$	$\delta^{p\text{Trw}}_{\text{cor}}$	$\delta^{\text{id}}_{\text{cor1}}$	$\delta^{\text{id}}_{\text{cor2}}$	$\delta^{\text{rec}}_{\text{cor}}$	$\delta^{\text{geant4}}_{\text{cor}}$	δ^{trig}	δ^{iso}	$\delta^{\text{res}}_{\text{unf}}$	δ^{MC}	$\delta^{\text{id}}_{\text{unc}}$	δ^{multijet}
[GeV]	[%]	[%]	[%]	[%]	[%]	[%]	[%]	[%]	[%]	[%]	[%]	[%]
26–31	−0.4	0.7	1.0	0.4	2.3	-1.2	0.6	1.4	1.8	2.2	1.2	3.9
31–36	−0.4	0.7	0.8	0.3	2.0	-1.2	0.5	1.1	1.0	1.7	1.1	3.6
36–41	−0.5	0.6	0.5	0.2	1.7	-1.2	0.3	0.8	0.9	1.7	0.8	3.2
41–46	−0.7	1.2	0.3	0.2	1.4	-1.2	0.3	0.6	1.1	1.9	0.6	3.1
46–51	−0.9	0.1	0.2	0.1	0.8	-1.2	0.2	0.4	1.2	2.1	0.4	2.8
51–56	−1.0	0.8	0.2	0.1	0.5	-1.2	0.2	0.3	1.4	2.0	0.3	2.3
56–61	−0.8	0.2	0.1	0.1	0.4	-1.2	0.1	0.2	1.5	1.6	0.3	2.0
61–66	−0.8	−0.9	0.1	0.1	0.3	-1.2	0.1	0.2	1.1	1.0	0.2	1.6

Table 2. The systematic uncertainties of the nominal electron-channel cross-section measurement. Some sources of uncertainty have both correlated and uncorrelated components. Correlated uncertainties arise from the uncertainty in the electroweak background contributions $\delta^{\text{e.w.}}_{\text{cor}}$, from corrections to the Monte Carlo modelling of the Z/γ^* p_{T} spectra, $\delta^{p\text{Trw}}_{\text{cor}}$, the electron identification efficiency, $\delta^{\text{id}}_{\text{cor1}}$ and $\delta^{\text{id}}_{\text{cor2}}$, the reconstruction efficiency, $\delta^{\text{rec}}_{\text{cor}}$, and from the Geant4 simulation, $\delta^{\text{geant4}}_{\text{cor}}$. Uncorrelated uncertainties arise from the isolation and trigger efficiency corrections, δ^{trig} and δ^{iso} respectively, unfolding uncertainties, $\delta^{\text{res}}_{\text{un}}$, and the statistical precision of the signal Monte Carlo, δ^{MC}. The electron identification efficiency uncertainties have several components other than the two largest correlated parts above and these are discussed in detail in ref. [19]. These additional components are all combined into a single uncorrelated error source $\delta^{\text{id}}_{\text{unc}}$. The uncertainty on the normalisation of the multijet background is given by δ^{multijet}. The luminosity uncertainty (1.8%) is not included.

$m_{\mu\mu}$	$\frac{\text{d}\sigma}{\text{d}m_{\mu\mu}}$	δ^{stat}	δ^{syst}	δ^{total}
[GeV]	[pb/GeV]	[%]	[%]	[%]
26–31	1.89	1.0	3.5	3.6
31–36	3.14	0.8	3.0	3.1
36–41	2.55	0.9	2.5	2.7
41–46	1.96	1.0	2.1	2.3
46–51	1.49	1.1	1.9	2.2
51–56	1.21	1.2	1.7	2.1
56–61	1.00	1.2	1.6	2.0
61–66	0.91	1.2	1.5	1.9

Table 3. The nominal muon-channel differential Born-level fiducial cross section, $\frac{\text{d}\sigma}{\text{d}m_{\mu\mu}}$. The statistical, δ^{stat}, systematic, δ^{syst} and total, δ^{total}, uncertainties are given for each invariant $m_{\mu\mu}$ mass bin. The luminosity uncertainty (1.8%) is not included.

JHEP06(2014)112

$m_{\mu\mu}$ [GeV]	Correlated $\delta^{\text{e.w.}}$ [%]	$\delta^{p\text{Trw}}$ [%]	$\delta^{\text{reco}}_{\text{cor}}$ [%]	$\delta^{\text{trig}}_{\text{cor}}$ [%]	$\delta^{\text{iso}}_{\text{cor}}$ [%]	δ^{multijet} [%]	$\delta^{p\text{T scale}}$ [%]	Uncorrelated $\delta^{\text{trig}}_{\text{unc}}$ [%]	$\delta^{\text{iso}}_{\text{unc}}$ [%]	δ^{res} [%]	δ^{MC} [%]	$\delta^{\text{reco}}_{\text{unc}}$ [%]
26–31	−0.1	-0.2	0.5	0.8	2.6	−1.1	−0.5	0.5	1.4	0.2	0.8	0.2
31–36	−0.1	0.2	0.5	0.8	2.1	−1.0	−0.8	0.5	1.2	0.1	0.6	0.2
36–41	−0.2	0.0	0.5	0.8	1.5	−0.8	−1.0	0.5	0.9	0.1	0.7	0.2
41–46	−0.3	-0.3	0.5	0.8	1.1	−0.8	−0.4	0.4	0.7	0.2	0.8	0.2
46–51	−0.4	-0.1	0.5	0.8	0.9	−0.5	−0.6	0.4	0.5	0.3	0.8	0.2
51–56	−0.4	-0.2	0.5	0.7	0.7	−0.5	−0.0	0.3	0.5	0.2	0.9	0.2
56–61	−0.4	-0.2	0.5	0.7	0.6	−0.4	−0.3	0.3	0.4	0.2	0.8	0.2
61–66	−0.3	-0.3	0.5	0.6	0.5	−0.3	0.9	0.2	0.3	0.2	0.3	0.2

Table 4. The systematic uncertainties for the nominal muon-channel cross-section measurement. Some sources of uncertainty have both correlated and uncorrelated components. Correlated uncertainties arise from the uncertainty in the electroweak background contributions $\delta^{\text{e.w.}}_{\text{cor}}$, from corrections to the Monte Carlo modelling of the Z/γ^* p_{T} spectra, and from the reconstruction, trigger and isolation efficiency corrections, given by $\delta^{\text{reco}}_{\text{cor}}$, $\delta^{\text{trig}}_{\text{cor}}$ and $\delta^{\text{iso}}_{\text{cor}}$ respectively. The uncertainty on the multijet and electroweak background cross sections, given by δ^{multijet} and $\delta^{\text{e.w.}}$ respectively and muon momentum scale uncertainty, $\delta^{p\text{T scale}}$, are also correlated. Uncorrelated uncertainties are due to corrections for the trigger and isolation efficiencies, given by $\delta^{\text{trig}}_{\text{unc}}$ and $\delta^{\text{iso}}_{\text{unc}}$ respectively. The uncertainty from the muon resolution correction, δ^{res}, from the size of the signal Monte Carlo sample, δ^{MC}, and the uncertaintities due to corrections for the reconstruction, $\delta^{\text{reco}}_{\text{unc}}$, are also uncorrelated. The luminosity uncertainty (1.8%) is not included.

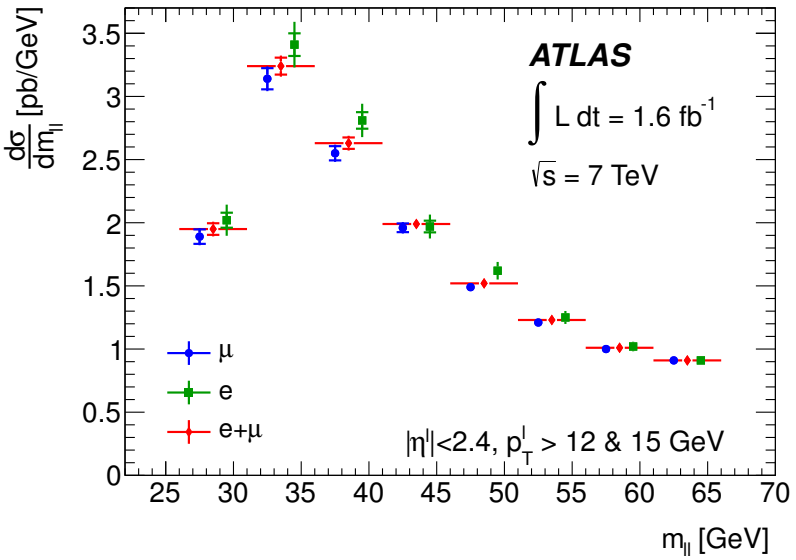

Figure 4. The fiducial Born-level combined e and μ channel cross section as well as the individual e channel and μ channel cross-section measurements as a function of the dilepton invariant mass, $m_{\ell\ell}$. The inner error bar represents the correlated systematic uncertainty and the outer error bar represents the total uncertainty in each bin. The electron and muon individual points are offset from the bin centre for the purposes of illustration. The luminosity uncertainty (1.8%) is not included.

JHEP06(2014)112

$m_{\ell\ell}$	$\frac{\mathrm{d}\sigma}{\mathrm{d}m_{\ell\ell}}$	δ^{stat}	δ^{cor}	δ^{unc}	δ^{tot}	δ_1^{cor}	δ_2^{cor}	δ_3^{cor}	δ_4^{cor}	δ_5^{cor}	δ_6^{cor}	δ_7^{cor}	δ_8^{cor}	δ_9^{cor}	$\delta_{10}^{\mathrm{cor}}$	$\delta_{11}^{\mathrm{cor}}$	$\delta_{12}^{\mathrm{cor}}$	$\delta_{13}^{\mathrm{cor}}$	$\mathcal{D}$	$\mathcal{A}$	$\delta_{\mathcal{A}}^{\mathrm{scale}}$	$\delta_{\mathcal{A}}^{\mathrm{pdf}+\alpha_s}$
[GeV]	[pb/GeV]	[%]	[%]	[%]	[%]	[%]	[%]	[%]	[%]	[%]	[%]	[%]	[%]	[%]	[%]	[%]	[%]	[%]			[%]	[%]
26–31	1.95	0.9	2.4	1.6	3.0	0.1	0.4	−1.2	0.7	−0.4	−0.6	0.4	0.5	−1.3	−0.0	−0.6	−0.3	0.8	0.98	0.069	$^{-4.2}_{+4.2}$	$^{-2.0}_{+1.4}$
31–36	3.24	0.7	2.1	1.4	2.6	0.1	0.3	−1.1	0.6	−0.3	−0.4	0.2	0.2	−1.1	−0.4	−0.4	−0.4	0.7	0.98	0.194	$^{-2.8}_{+3.6}$	$^{-1.6}_{+1.1}$
36–41	2.63	0.8	1.7	1.2	2.2	0.2	0.2	−1.0	0.5	−0.2	−0.2	0.3	0.3	−0.8	−0.6	−0.2	−0.3	0.5	0.99	0.270	$^{-1.2}_{+1.1}$	$^{-1.4}_{+0.9}$
41–46	1.99	0.9	1.4	1.1	2.0	0.2	0.2	−1.0	0.4	−0.2	−0.0	0.3	0.4	−0.5	−0.2	−0.2	−0.0	0.4	1.00	0.321	$^{-1.2}_{+1.0}$	$^{-1.2}_{+0.8}$
46–51	1.52	0.9	1.2	1.1	1.9	0.2	0.3	−0.8	0.4	−0.1	0.1	0.2	0.3	−0.4	−0.3	−0.0	−0.2	0.4	1.05	0.356	$^{-0.9}_{+0.6}$	$^{-1.0}_{+0.7}$
51–56	1.23	1.0	1.1	1.0	1.8	0.2	0.3	−0.8	0.3	−0.1	0.1	0.2	0.2	−0.2	−0.0	−0.2	0.1	0.3	1.11	0.381	$^{-0.4}_{+0.5}$	$^{-1.0}_{+0.6}$
56–61	1.01	1.0	1.0	1.0	1.7	0.3	0.3	−0.7	0.3	−0.1	0.2	0.2	0.2	−0.2	−0.1	−0.1	−0.1	0.2	1.19	0.406	$^{-0.9}_{+0.3}$	$^{-0.9}_{+0.6}$
61–66	0.91	1.0	1.1	0.6	1.6	0.3	0.3	−0.6	0.3	−0.0	0.2	0.1	0.1	−0.0	0.7	−0.1	0.2	0.1	1.30	0.427	$^{-0.6}_{+0.4}$	$^{-0.8}_{+0.5}$

Table 5. The combined Born-level fiducial differential cross section $\frac{d\sigma}{dm_{\ell\ell}}$, statistical δ^{stat}, total correlated δ^{cor}, uncorrelated δ^{unc}, and total δ^{total} uncertainties, as well as individual correlated sources δ_i^{cor}. The correlated uncertainties are a linear combination of the 13 correlated uncertainties in the nominal muon and electron channels. As the uncertainties on the combined result no longer originate from individual error sources they are numbered 1–13. Also shown is the correction factor used to derive the dressed cross section ($\mathcal{D}$), and the NNLO extrapolation factor ($\mathcal{A}$) used to derive the cross section for the full phase space, along with the uncertainties associated to variations in scale choice $\delta_{\mathcal{A}}^{\mathrm{scale}}$, and PDF uncertainty $\delta_{\mathcal{A}}^{\mathrm{pdf}+\alpha_s}$. The luminosity uncertainty (1.8%) is not included.

$m_{\ell\ell}$ [GeV]	$\frac{d\sigma}{dm_{\ell\ell}}$ [pb/GeV]	δ^{stat} [%]	δ^{syst} [%]	δ^{tot} [%]	$\mathcal{D}$	$\mathcal{A}$	$\delta_{\mathcal{A}}^{\text{scale}}$ [%]	$\delta_{\mathcal{A}}^{\text{pdf}+\alpha_s}$ [%]
12–17	12.41	4.2	12.6	13.3	1.00	0.04	$^{-7.1}_{+7.5}$	$^{-4.1}_{+2.7}$
17–22	22.57	3.1	12.3	12.7	0.98	0.20	$^{-3.7}_{+4.2}$	$^{-3.0}_{+2.0}$
22–28	14.64	3.3	9.5	10.0	0.98	0.30	$^{-0.4}_{+0.8}$	$^{-2.3}_{+1.6}$
28–36	6.73	4.0	7.4	8.5	0.99	0.35	$^{-0.3}_{+0.3}$	$^{-1.8}_{+1.2}$
36–46	2.81	5.2	5.7	7.8	1.02	0.39	$^{-0.3}_{+0.4}$	$^{-1.3}_{+0.9}$
46–66	1.27	4.7	5.2	7.1	1.16	0.43	$^{-0.4}_{+0.7}$	$^{-1.0}_{+0.6}$

Table 6. The extended muon channel Born-level fiducial differential cross section $\frac{d\sigma}{dm_{\ell\ell}}$, with the statistical δ^{stat}, systematic δ^{syst}, and total δ^{tot} uncertainties for each invariant mass bin. Also shown is the correction factor used to derive the dressed cross section ($\mathcal{D}$), and the extrapolation factor ($\mathcal{A}$) used to derive the cross section for the full phase space, along with the uncertainties associated to variations in scale $\delta_{\mathcal{A}}^{\text{scale}}$, and PDF uncertainty $\delta_{\mathcal{A}}^{\text{pdf}+\alpha_s}$. The luminosity uncertainty (3.5%) is not included.

In addition to the combined fiducial cross sections, table 5 also provides two factors to obtain the dressed-level fiducial cross sections and to extrapolate the Born cross sections to the full kinematic range. The former is determined by multiplying the fiducial cross section by the dressed correction factor $\mathcal{D}$, and the latter is determined by dividing the fiducial cross section by the acceptance $\mathcal{A}$ as defined in section 3.4. Both factors are obtained from MC simulation.

The acceptance correction is determined at NNLO in QCD using the FEWZ program and is found to be sizeable at low $m_{\ell\ell}$, with a correction factor of 0.069 in the lowest mass bin, but increasing rapidly with increasing $m_{\ell\ell}$. The low acceptance is largely driven by the lepton p_T^{ℓ} cuts. The calculation is subject to additional theoretical uncertainties arising from the choice of renormalisation and factorisation scales, μ_R and μ_F respectively, and the choice of PDFs used in the calculation. The scales are varied simultaneously by factors of two with respect to the default scale choice of $\mu_R = \mu_F = m_{\ell\ell}$. The variation is taken as an estimate of the uncertainty, which is found to be $\sim 1\%$ reaching $\sim 4\%$ at low $m_{\ell\ell}$. The PDF uncertainty is taken from the MSTW2008 NNLO PDFs by taking the quadratic sum of cross-section shifts using the 68% confidence level (CL) eigenvectors and α_s variations [17] and is found to be 1–2%.

4.2 Low-mass extended analysis

The measurements of the Born-level fiducial cross section in the extended analysis are given in table 6, which also includes the dressed correction factor $\mathcal{D}$, and the acceptance $\mathcal{A}$ along with its uncertainties. The complete breakdown of the systematic uncertainty contributions is given in table 7. The dominant sources of systematic uncertainty in this measurement are due to the trigger efficiency and the efficiency of the isolation requirement.

The measurements of the nominal and extended analyses cannot be compared directly due to the different fiducial regions. A comparison of the Born-level extrapolated mea-

JHEP06(2014)112

$m_{\mu\mu}$ [GeV]	Correlated δ^{reco} [%]	δ^{trig} [%]	δ^{iso} [%]	δ^{multijet} [%]	$\delta^{p\text{T scale}}$ [%]	Uncorrelated δ^{res} [%]	δ^{MC} [%]
12–17	2.5	4.0	11.3	−3.0	−0.2	0.5	0.6
17–22	1.4	3.7	11.3	−2.8	0.1	0.3	0.3
22–28	0.9	3.6	8.5	−1.8	0.0	0.1	0.4
28–36	0.7	3.6	6.2	−1.6	−0.1	0.2	0.4
36–46	0.7	3.6	4.2	−1.3	−0.1	0.1	0.5
46–66	0.6	3.6	3.6	−0.7	−0.0	0.1	0.5

Table 7. The systematic uncertainties for the extended muon channel cross-section measurement in each invariant mass bin. Correlated uncertainties come from the reconstruction, trigger and isolation efficiency corrections, given by δ^{reco}, δ^{trig} and δ^{iso} respectively. The uncertainty on the multijet background cross section, δ^{multijet} and the uncertainty on the muon momentum scale, $\delta^{p\text{T scale}}$, are also correlated across bins. Uncorrelated uncertainties are due to the uncertainty from the muon resolution correction, δ^{res}, and the sample size of the signal Monte Carlo sample, δ^{MC}.The luminosity uncertainty (3.5%) is not included.

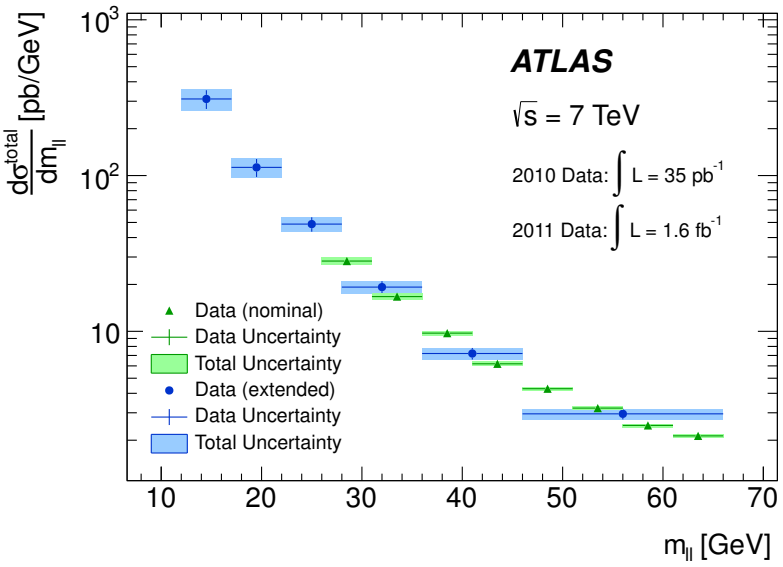

Figure 5. Comparison of Born-level nominal $(e+\mu)$ and extended (μ) channel differential cross sections as a function of the dilepton invariant mass, $m_{\ell\ell}$, extrapolated to full phase space. The data uncertainties are the total fiducial cross-section uncertainties, while the total uncertainties also include theoretical uncertainties from the acceptance correction. The luminosity uncertainties (nominal 1.8%, extended 3.5%) are included in the error band.

surements, $\mathrm{d}\sigma^{\text{total}}/\mathrm{d}m_{\ell\ell}$, determined by application of the acceptance correction factors is shown in figure 5. The two measurements are in good agreement with each other and show the expected rapid decrease of the cross section with increasing $m_{\ell\ell}$.

JHEP06(2014)112

4.3 Theory comparison

The fiducial cross-section measurements are compared to theoretical predictions from FEWZ at NLO and NNLO as well as NLO calculations matched to a LL resummed parton shower calculation from POWHEG. In order to compare the QCD calculations to the data, additional corrections are required to account for higher-order electroweak radiative effects [56] and photon induced processes, $\gamma\gamma \to \ell\ell$ [57]. The calculations are performed using FEWZ and cross checked with SANC [44].

The electroweak corrections calculated in the G_μ scheme, Δ^{HOEW}, account for the effects of pure weak-vertex and self-energy corrections, double boson exchange, initial-state radiation (ISR), and the interference between ISR and FSR. A comparison of the HOEW corrections obtained with the alternative $\alpha(M_Z)$ electroweak scheme [43], $\Delta^{\mathrm{HOEW}}_{\alpha(M_Z)}$, yields different results at low $m_{\ell\ell}$ and the difference, δ^{scheme}, is listed in tables 10 and 11, where $\Delta^{\mathrm{HOEW}} = \Delta^{\mathrm{HOEW}}_{\alpha(M_Z)} - \delta^{\mathrm{scheme}}$.

The cross-section contribution from photon induced processes, Δ^{PI}, is estimated using the MRST2004QED PDF set [58] in which photon radiation from the quark lines is included in the parton evolution equations. The cross-section predictions are calculated using the NLO and NNLO MSTW2008 sets as appropriate. The full cross-section predictions including all corrections are shown in tables 8 and 9 for nominal and extended analysis respectively. The corrections and associated uncertainties are also listed in tables 10 and 11 for both fiducial measurements. The Δ^{PI} corrections contribute 2–3% of the theoretical predictions.

The comparisons between the measured cross sections and the theoretical predictions are shown in figure 6. The FEWZ NLO predictions provide a poor description of the data at low $m_{\ell\ell}$ which simultaneously overestimates and underestimates the nominal and extended measurements respectively. The POWHEG predictions differ from FEWZ by as much as 20% and describe the data well. These calculations have an uncertainty dominated by the scale variations which can reach 10% to 20% in the lowest $m_{\ell\ell}$ bin for each fiducial measurement. Such relatively large scale effects at NLO can arise since the region of $m_{\ell\ell} \sim 2p^{\ell}_{\mathrm{T}}$ is only populated by NLO type events leading to unusually large scale variations. The POWHEG calculations absorb resummed LL parton shower effects, which improve the prediction in this region. At NNLO the pure fixed-order FEWZ predictions also compare well with the measured fiducial cross sections. The associated scale uncertainties are in this case much smaller, but still at the level of 5% in the lowest bin of nominal, and 10% in the lowest bin of extended measurements, respectively.

To quantify the level of agreement between the measured cross sections and the predictions, the value of the χ^2 function is calculated taking into account the correlated experimental systematic uncertainties as well as the theoretical uncertainties arising from the PDFs and scale variations. The χ^2 function is defined as in ref. [16] and the results are shown in table 12.

The values of the χ^2 function obtained with MSTW2008 PDFs are good when compared to POWHEG or FEWZ at NNLO; however the FEWZ NLO prediction yields very large values. Thus, the measured cross sections are significantly more compatible with the NNLO prediction than with the NLO prediction.

JHEP06(2014)112

$m_{\ell\ell}$ [GeV]	POWHEG $\frac{d\sigma}{dm_{\ell\ell}}$ [pb/GeV]	POWHEG δ^{pdf} [%]	POWHEG δ^{scale} [%]	FEWZ NLO $\frac{d\sigma}{dm_{\ell\ell}}$ [pb/GeV]	FEWZ NLO δ^{pdf} [%]	FEWZ NLO δ^{scale} [%]	FEWZ NNLO $\frac{d\sigma}{dm_{\ell\ell}}$ [pb/GeV]	FEWZ NNLO δ^{pdf} [%]	FEWZ NNLO δ^{scale} [%]
26–31	1.80	2.5	$^{+\ 7.3}_{-11.4}$	2.22	2.7	$^{+4.9}_{-7.9}$	1.93	$^{+3.5}_{-2.7}$	5.7
31–36	3.12	2.4	$^{+\ 5.3}_{-10.0}$	3.49	2.7	$^{+4.7}_{-6.3}$	3.04	$^{+3.2}_{-2.5}$	4.5
36–41	2.64	2.3	$^{+4.6}_{-8.8}$	2.69	2.6	$^{+4.1}_{-5.0}$	2.58	$^{+3.1}_{-2.4}$	2.3
41–46	2.03	2.2	$^{+3.5}_{-7.5}$	2.00	2.6	$^{+3.6}_{-4.2}$	1.98	$^{+3.1}_{-2.3}$	2.1
46–51	1.54	1.9	$^{+3.7}_{-6.1}$	1.50	2.5	$^{+3.2}_{-3.5}$	1.51	$^{+3.0}_{-2.2}$	1.7
51–56	1.19	2.4	$^{+4.5}_{-5.1}$	1.17	2.4	$^{+2.8}_{-2.9}$	1.18	$^{+2.9}_{-2.2}$	1.3
56–61	1.00	2.4	$^{+2.3}_{-4.7}$	0.97	2.4	$^{+2.6}_{-2.6}$	0.98	$^{+2.9}_{-2.1}$	1.3
61–66	0.90	2.1	$^{+2.0}_{-4.5}$	0.87	2.3	$^{+2.3}_{-2.3}$	0.88	$^{+2.8}_{-2.1}$	1.2

Table 8. Theory predictions for NLO+LLPS and for fixed-order calculations at NLO and NNLO including higher-order electroweak corrections, for the nominal analysis of the differential cross section $\frac{d\sigma}{dm_{\ell\ell}}$ as a function of the invariant mass $m_{\ell\ell}$. The scale uncertainty is defined as the envelope of variations for $0.5 \leq \mu_R, \mu_F \leq 2$ for POWHEG. For FEWZ the scale uncertainty is defined by the variation $0.5 \leq \mu_R = \mu_F \leq 2$.

$m_{\mu\mu}$ [GeV]	POWHEG $\frac{d\sigma}{dm_{\mu\mu}}$ [pb/GeV]	POWHEG δ^{pdf} [%]	POWHEG δ^{scale} [%]	FEWZ NLO $\frac{d\sigma}{dm_{\mu\mu}}$ [pb/GeV]	FEWZ NLO δ^{pdf} [%]	FEWZ NLO δ^{scale} [%]	FEWZ NNLO $\frac{d\sigma}{dm_{\mu\mu}}$ [pb/GeV]	FEWZ NNLO $\delta^{pdf+\alpha_s}$ [%]	FEWZ NNLO δ^{scale} [%]
12–17	9.88	2.3	$^{+12.3}_{-20.9}$	7.47	2.7	$^{+10.7}_{-15.8}$	12.09	$^{+3.7}_{-3.0}$	10.0
17–22	20.99	2.6	$^{+\ 8.4}_{-15.6}$	24.46	3.0	$^{+10.1}_{-13.3}$	21.22	$^{+3.7}_{-2.8}$	6.1
22–28	13.69	2.6	$^{+\ 5.5}_{-12.1}$	13.65	2.9	$^{+6.2}_{-8.6}$	13.56	$^{+3.4}_{-2.6}$	2.3
28–36	6.92	2.3	$^{+\ 6.2}_{-10.8}$	6.61	2.7	$^{+5.0}_{-6.5}$	6.74	$^{+3.3}_{-2.5}$	1.3
36–46	3.18	2.3	$^{+4.4}_{-8.6}$	3.01	2.6	$^{+4.0}_{-4.4}$	3.10	$^{+3.1}_{-2.3}$	1.2
46–66	1.31	2.2	$^{+2.9}_{-5.7}$	1.24	2.4	$^{+2.8}_{-3.0}$	1.28	$^{+2.9}_{-2.1}$	1.3

Table 9. Theory predictions for NLO+LLPS and for fixed-order calculations at NLO and NNLO including higher-order electroweak corrections, for the extended analysis of the differential cross section $\frac{d\sigma}{dm_{\ell\ell}}$ as a function of the invariant mass $m_{\ell\ell}$. The scale uncertainty is defined as the envelope of variations for $0.5 \leq \mu_R, \mu_F \leq 2$ for POWHEG. For FEWZ the scale uncertainty is defined by the variation $0.5 \leq \mu_R = \mu_F \leq 2$.

JHEP06(2014)112

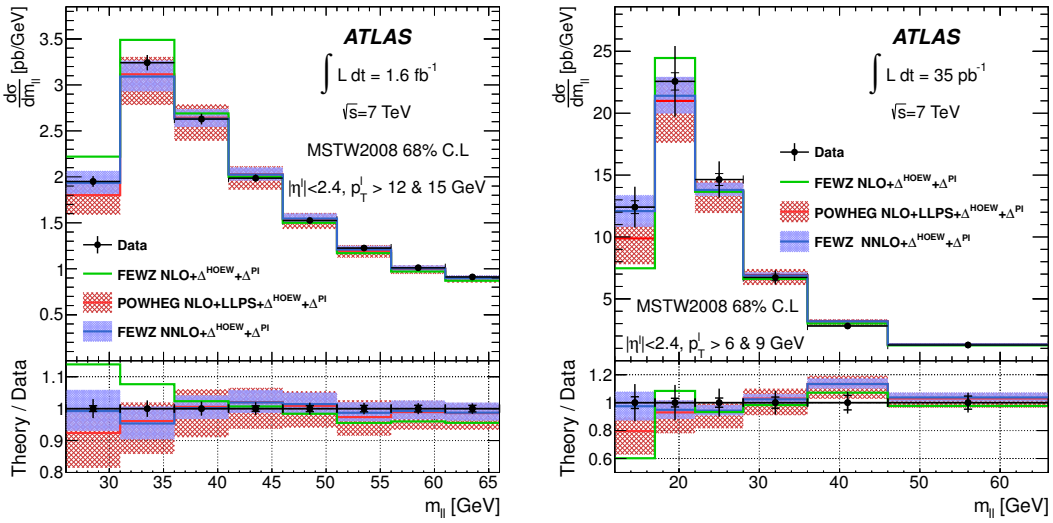

(a) **(b)**

Figure 6. The measured fiducial differential cross section, $\frac{d\sigma}{dm_{\ell\ell}}$ for (a) the nominal analysis and (b) the extended analysis as a function of the invariant mass $m_{\ell\ell}$ (solid points) compared to NLO predictions from FEWZ, NLO+LLPS predictions from POWHEG and NNLO predictions from FEWZ (all including higher-order electroweak and photon induced corrections). The predictions are calculated using MSTW2008 PDF sets with the appropriate order of perturbative QCD. The uncertainty bands include the PDF and α_s variations at 68% CL, scale variations between 0.5 and 2 times the nominal scales, and the uncertainty in the PI correction. The ratios of all three theoretical predictions (solid lines) to the data are shown in the lower panels. The data (solid points) are displayed at unity with the statistical (inner) and total (outer) measurement uncertainties.

$m_{\ell\ell}$ [GeV]	Δ^{HOEW} [%]	Δ^{PI} [pb/GeV]	δ^{scheme} [%]
$26-31$	1.10	0.005 ± 0.002	$+4.6$
$31-36$	3.10	0.051 ± 0.018	$+1.5$
$36-41$	3.92	0.053 ± 0.019	$+0.8$
$41-46$	4.25	0.045 ± 0.016	$+0.5$
$46-51$	4.46	0.036 ± 0.013	$+0.4$
$51-56$	4.43	0.029 ± 0.010	$+0.4$
$56-61$	4.47	0.023 ± 0.008	$+0.3$
$61-66$	4.09	0.019 ± 0.007	$+0.4$

Table 10. Higher-order electroweak corrections in nominal analysis, Δ^{HOEW}, and the correction for the Photon Induced process, Δ^{PI}, together with its uncertainty derived from the uncertainty of the photon PDF as a function of the dilepton invariant mass $m_{\ell\ell}$. Also shown is the difference arising from the non-convergence of calculations derived with different electroweak schema, δ^{scheme}.

JHEP06(2014)112

$m_{\ell\ell}$ [GeV]	Δ^{HOEW} [%]	Δ^{PI} [pb/GeV]	δ^{scheme} [%]
$12-17$	0.37	0.000 ± 0.000	+5.4
$17-22$	1.58	0.190 ± 0.070	+3.2
$22-28$	3.04	0.240 ± 0.087	+0.9
$28-36$	3.77	0.150 ± 0.054	+0.5
$36-46$	4.38	0.085 ± 0.030	+0.3
$46-66$	4.64	0.037 ± 0.013	+0.2

Table 11. Higher-order electroweak corrections in extended analysis, Δ^{HOEW}, and the correction for the Photon Induced process, Δ^{PI}, together with its uncertainty derived from the uncertainty of the photon PDF as a function of the dilepton invariant mass $m_{\ell\ell}$. Also shown is the difference arising from the non-convergence of calculations derived with different electroweak schema, δ^{scheme}.

Prediction	χ^2 (8 points) Nominal	χ^2 (6 points) Extended
POWHEG NLO+LLPS	22.4 (19.8)	22.3 (18.6)
FEWZ NLO	48.7 (28.6)	139.7 (133.7)
FEWZ NNLO	13.9 (12.9)	7.1 (7.1)

Table 12. Values of χ^2 for the nominal and extended DY cross-section measurements for predictions based from FEWZ at NLO and NNLO and POWHEG using MSTW2008 PDFs accounting for the experimental correlated systematic uncertainties. The values in the brackets show the χ^2 when the PDF and scale uncertainties on the theoretical predictions are taken into account.

Prediction	χ^2 (8 points) Nominal	χ^2 (6 points) Extended
NLO Fit	40.7	117.1
NNLO Fit	8.5	7.8

Table 13. The χ^2 values from NLO and NNLO QCD fits made using the ATLAS nominal and extended Drell-Yan cross-section measurements and the HERA-I dataset accounting for the experimental correlated systematic uncertainties.

To investigate to what extent the disagreement with a pure NLO calculation is dependent on the PDF used, a QCD analysis of the data is performed. In this analysis the χ^2 function is evaluated after fitting the PDFs to deep inelastic scattering data from HERA [16] and the new measurements presented here. The QCD fit is performed using MCFM [59] and APPLGRID [60] in the HERAFitter framework [16, 61–67] at NLO and at NNLO using additional NNLO K-factors obtained from FEWZ. The PDFs are parameterised using functional forms described in ref. [68] where terms are added in the polynomial expansion of the PDFs only if required by the data, following the procedure described in

JHEP06(2014)112

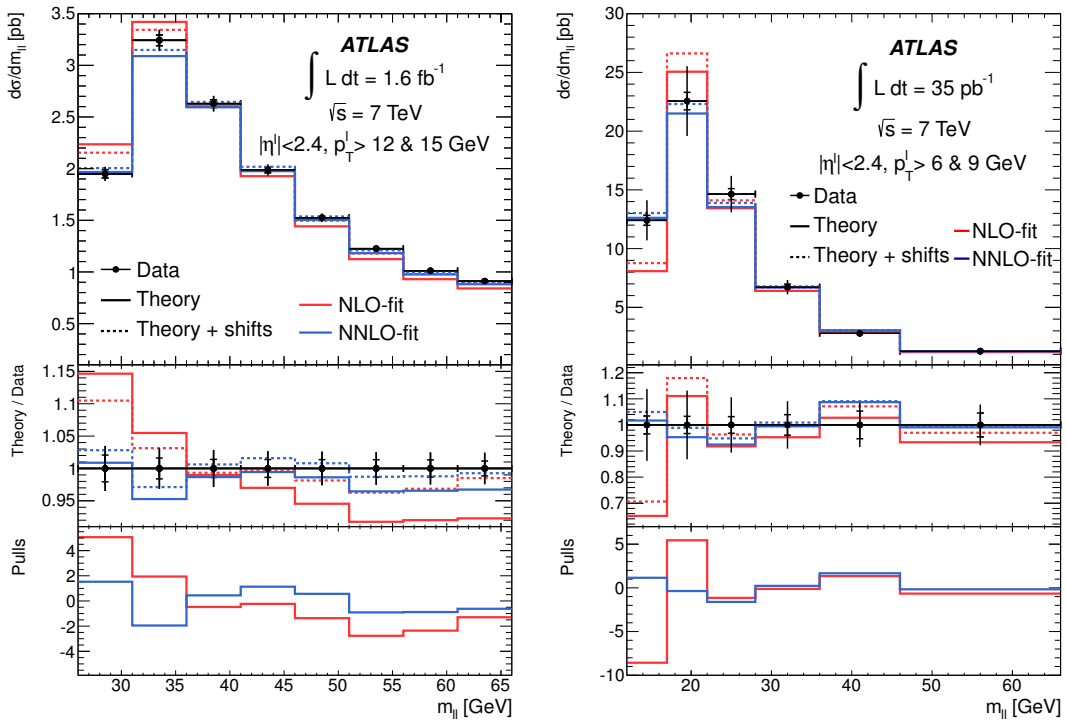

(a) **(b)**

Figure 7. The measured differential cross section $\frac{d\sigma}{dm_{\ell\ell}}$ for (a) the nominal and (b) the extended-analysis as a function of invariant mass $m_{\ell\ell}$ compared to the NLO and NNLO QCD fits (solid lines). The inner error bars show the total uncorrelated experimental uncertainty, and the outer error bars represent the total experimental uncertainty, excluding the luminosity uncertainties. The dashed lines correspond to the QCD fit after applying the adjustments of the fitted nuisance parameters for each correlated error source. The lower half of each figure shows the ratio of theory expectations to data in the upper part, and the χ^2 pull contribution in the lower part.

ref. [16]. The data are then included in the χ^2 function, which is minimised with respect to the PDF parameters. The NLO and NNLO QCD fits using only HERA data yield acceptable fits with $\chi^2/\text{dof} = 468.3/537$ and $\chi^2/\text{dof} = 466.3/537$ respectively. When the new ATLAS measurements are included the NLO fit is unable to describe the data and the total χ^2 value for these measurements, taking into account 20 sources of correlated uncertainty, is 158 for 14 data points. However, the QCD analysis performed at NNLO results in a good fit with a total χ^2 value of 16.3 for 14 measurements.

The results of the analysis are given in table 13 and figure 7 where the NLO and NNLO QCD fit results are shown in the upper panels and compared to the nominal and extended analysis measurements. Also shown are the results of the fit after applying the adjustments of the fitted nuisance parameters for each correlated error source. The central panels shows the ratio of theory to data, and the lower panel shows the χ^2 pull for each measurement bin. The pulls for the NLO fit are large at low invariant masses as expected from the phase space constraints created by the transverse momentum cuts applied to the leptons. However, there are also large pulls for the higher invariant masses.

JHEP06(2014)112

5 Conclusion

The differential cross section $\mathrm{d}\sigma/\mathrm{d}m_{\ell\ell}$ for the Drell-Yan production of dileptons is measured by ATLAS in pp collisions at $\sqrt{s} = 7\,\mathrm{TeV}$ at the LHC. The measurements are performed using di-electron and di-muon events in a nominal fiducial region using $1.6\,\mathrm{fb}^{-1}$ of integrated luminosity from 2011 covering the range $26 < m_{\ell\ell} < 66\,\mathrm{GeV}$ and $|\eta| < 2.4$. The measurement is also performed using di-muon events in an extended fiducial region covering the range $12 < m_{\ell\ell} < 66\,\mathrm{GeV}$ and $|\eta| < 2.4$ using $35\ \mathrm{pb}^{-1}$ of integrated luminosity from 2010.

The fiducial cross sections are compared to fixed order theoretical predictions at NLO and NNLO from FEWZ, as well as an NLO with matched leading-logarithm parton shower calculation from POWHEG. The calculations are corrected for additional higher-order electroweak radiative effects including a photon induced term. Using renormalisation and factorisation scales equal to $m_{\ell\ell}$, the pure NLO prediction using the MSTW2008 PDF yields a very large χ^2 value, whereas both the NNLO and NLO matched to leading logarithm parton shower predictions provide good descriptions of the data. The results are supported by a QCD analysis of the measurements performed at NLO and NNLO. The PDFs are fitted to the new measurements together with inclusive ep measurements from HERA. The NNLO fit performs significantly better than the NLO fit in describing the data.

Acknowledgments

We thank CERN for the very successful operation of the LHC, as well as the support staff from our institutions without whom ATLAS could not be operated efficiently.

We acknowledge the support of ANPCyT, Argentina; YerPhI, Armenia; ARC, Australia; BMWF and FWF, Austria; ANAS, Azerbaijan; SSTC, Belarus; CNPq and FAPESP, Brazil; NSERC, NRC and CFI, Canada; CERN; CONICYT, Chile; CAS, MOST and NSFC, China; COLCIENCIAS, Colombia; MSMT CR, MPO CR and VSC CR, Czech Republic; DNRF, DNSRC and Lundbeck Foundation, Denmark; EPLANET, ERC and NSRF, European Union; IN2P3-CNRS, CEA-DSM/IRFU, France; GNSF, Georgia; BMBF, DFG, HGF, MPG and AvH Foundation, Germany; GSRT and NSRF, Greece; ISF, MINERVA, GIF, I-CORE and Benoziyo Center, Israel; INFN, Italy; MEXT and JSPS, Japan; CNRST, Morocco; FOM and NWO, Netherlands; BRF and RCN, Norway; MNiSW and NCN, Poland; GRICES and FCT, Portugal; MNE/IFA, Romania; MES of Russia and ROSATOM, Russian Federation; JINR; MSTD, Serbia; MSSR, Slovakia; ARRS and MIZŠ, Slovenia; DST/NRF, South Africa; MINECO, Spain; SRC and Wallenberg Foundation, Sweden; SER, SNSF and Cantons of Bern and Geneva, Switzerland; NSC, Taiwan; TAEK, Turkey; STFC, the Royal Society and Leverhulme Trust, United Kingdom; DOE and NSF, United States of America.

The crucial computing support from all WLCG partners is acknowledged gratefully, in particular from CERN and the ATLAS Tier-1 facilities at TRIUMF (Canada), NDGF (Denmark, Norway, Sweden), CC-IN2P3 (France), KIT/GridKA (Germany), INFN-CNAF (Italy), NL-T1 (Netherlands), PIC (Spain), ASGC (Taiwan), RAL (U.K.) and BNL (U.S.A.) and in the Tier-2 facilities worldwide.

JHEP06(2014)112

References

[1] S.D. Drell and T.-M. Yan, *Massive lepton pair production in hadron-hadron collisions at high-energies*, *Phys. Rev. Lett.* **25** (1970) 316 [*Erratum ibid.* **25** (1970) 902] [INSPIRE].

[2] E. Perez and E. Rizvi, *The quark and gluon structure of the proton*, *Rep. Prog. Phys.* **76** (2013) 046201 [arXiv:1208.1178] [INSPIRE].

[3] ATLAS collaboration, *Measurement of the inclusive $W^{\pm}$ and Z/γ cross sections in the electron and muon decay channels in pp collisions at $\sqrt{s} = 7$ TeV with the ATLAS detector*, *Phys. Rev.* **D 85** (2012) 072004 [arXiv:1109.5141] [INSPIRE].

[4] ATLAS collaboration, *Measurement of the high-mass Drell-Yan differential cross-section in pp collisions at $\sqrt{s} = 7$ TeV with the ATLAS detector*, *Phys. Lett.* **B 725** (2013) 223 [arXiv:1305.4192] [INSPIRE].

[5] CMS collaboration, *Measurement of the inclusive W and Z production cross sections in pp collisions at $\sqrt{s} = 7$ TeV*, *JHEP* **10** (2011) 132 [arXiv:1107.4789] [INSPIRE].

[6] CMS collaboration, *Measurement of the Drell-Yan cross section in pp collisions at $\sqrt{s} = 7$ TeV*, *JHEP* **10** (2011) 007 [arXiv:1108.0566] [INSPIRE].

[7] CMS collaboration, *Measurement of the differential and double-differential Drell-Yan cross sections in proton-proton collisions at $\sqrt{s} = 7$ TeV*, *JHEP* **12** (2013) 030 [arXiv:1310.7291] [INSPIRE].

[8] LHCb collaboration, *Inclusive W and Z production in the forward region at $\sqrt{s} = 7$ TeV*, *JHEP* **06** (2012) 058 [arXiv:1204.1620] [INSPIRE].

[9] LHCb collaboration, *Measurement of the cross-section for $Z \to e^+e^-$ production in pp collisions at $\sqrt{s} = 7$ TeV*, *JHEP* **02** (2013) 106 [arXiv:1212.4620] [INSPIRE].

[10] R. Hamberg, W.L. van Neerven and T. Matsuura, *A complete calculation of the order α_s^2 correction to the Drell-Yan K factor*, *Nucl. Phys.* **B 359** (1991) 343 [*Erratum ibid.* **B 644** (2002) 403] [INSPIRE].

[11] S. Catani, L. Cieri, G. Ferrera, D. de Florian and M. Grazzini, *Vector boson production at hadron colliders: a fully exclusive QCD calculation at NNLO*, *Phys. Rev. Lett.* **103** (2009) 082001 [arXiv:0903.2120] [INSPIRE].

[12] S. Catani and M. Grazzini, *An NNLO subtraction formalism in hadron collisions and its application to Higgs boson production at the LHC*, *Phys. Rev. Lett.* **98** (2007) 222002 [hep-ph/0703012] [INSPIRE].

[13] K. Melnikov and F. Petriello, *Electroweak gauge boson production at hadron colliders through $\mathcal{O}(\alpha_s^2)$*, *Phys. Rev.* **D 74** (2006) 114017 [hep-ph/0609070] [INSPIRE].

[14] S. Frixione and B.R. Webber, *Matching NLO QCD computations and parton shower simulations*, *JHEP* **06** (2002) 029 [hep-ph/0204244] [INSPIRE].

[15] S. Alioli, P. Nason, C. Oleari and E. Re, *NLO vector-boson production matched with shower in POWHEG*, *JHEP* **07** (2008) 060 [arXiv:0805.4802] [INSPIRE].

JHEP06(2014)112

[16] H1 and ZEUS collaborations, F.D. Aaron et al., *Combined measurement and QCD analysis of the inclusive $e^{\pm}p$ scattering cross sections at HERA*, *JHEP* **01** (2010) 109 [arXiv:0911.0884] [INSPIRE].

[17] A.D. Martin, W.J. Stirling, R.S. Thorne and G. Watt, *Parton distributions for the LHC*, *Eur. Phys. J.* **C 63** (2009) 189 [arXiv:0901.0002] [INSPIRE].

[18] ATLAS collaboration, *The ATLAS experiment at the CERN Large Hadron Collider*, 2008 *JINST* **3** S08003 [INSPIRE].

[19] ATLAS collaboration, *Electron reconstruction and identification efficiency measurements with the ATLAS detector using the* 2011 *LHC proton-proton collision data*, ATLAS-PERF-2013-03-001, CERN, Geneva Switzerland (2013).

[20] T. Sjöstrand, S. Mrenna and P.Z. Skands, *PYTHIA* 6.4 *physics and manual*, *JHEP* **05** (2006) 026 [hep-ph/0603175] [INSPIRE].

[21] A. Sherstnev and R.S. Thorne, *Parton distributions for LO generators*, *Eur. Phys. J.* **C 55** (2008) 553 [arXiv:0711.2473] [INSPIRE].

[22] L. Dixon, *A program for computing rapidity distributions for production of lepton-pairs via virtual photons, W or Z bosons at hadron colliders at NNLO in QCD*, http://www.slac.stanford.edu/~lance/Vrap/, July 2010.

[23] M. Cacciari, M. Czakon, M. Mangano, A. Mitov and P. Nason, *Top-pair production at hadron colliders with next-to-next-to-leading logarithmic soft-gluon resummation*, *Phys. Lett.* **B 710** (2012) 612 [arXiv:1111.5869] [INSPIRE].

[24] P. Bärnreuther, M. Czakon and A. Mitov, *Percent level precision physics at the Tevatron: first genuine NNLO QCD corrections to $q\bar{q} \to t\bar{t} + X$*, *Phys. Rev. Lett.* **109** (2012) 132001 [arXiv:1204.5201] [INSPIRE].

[25] M. Czakon and A. Mitov, *NNLO corrections to top pair production at hadron colliders: the quark-gluon reaction*, *JHEP* **01** (2013) 080 [arXiv:1210.6832] [INSPIRE].

[26] M. Czakon and A. Mitov, *NNLO corrections to top-pair production at hadron colliders: the all-fermionic scattering channels*, *JHEP* **12** (2012) 054 [arXiv:1207.0236] [INSPIRE].

[27] M. Czakon, P. Fiedler and A. Mitov, *Total top-quark pair-production cross section at hadron colliders through $O(\alpha_s^4)$*, *Phys. Rev. Lett.* **110** (2013) 252004 [arXiv:1303.6254] [INSPIRE].

[28] M. Czakon and A. Mitov, *Top++: a program for the calculation of the top-pair cross-section at hadron colliders*, arXiv:1112.5675 [INSPIRE].

[29] G. Corcella et al., *HERWIG* 6*: an event generator for hadron emission reactions with interfering gluons (including supersymmetric processes)*, *JHEP* **01** (2001) 010 [hep-ph/0011363] [INSPIRE].

[30] N. Davidson, G. Nanava, T. Przedzinski, E. Richter-Was and Z. Was, *Universal interface of TAUOLA technical and physics documentation*, *Comput. Phys. Commun.* **183** (2012) 821 [arXiv:1002.0543] [INSPIRE].

[31] P. Golonka and Z. Was, *PHOTOS Monte Carlo: a precision tool for QED corrections in Z and W decays*, *Eur. Phys. J.* **C 45** (2006) 97 [hep-ph/0506026] [INSPIRE].

[32] ATLAS collaboration, *Charged particle multiplicities in pp interactions at $\sqrt{s} = 0.9$ and 7 TeV in a diffractive limited phase-space measured with the ATLAS detector at the LHC and new PYTHIA* 6 *tune*, ATLAS-CONF-2010-031, CERN, Geneva Switzerland (2010).

JHEP06(2014)112

[33] ATLAS collaboration, *ATLAS tunes of PYTHIA 6 and PYTHIA 8 for MC11*, ATL-PHYS-PUB-2011-009, CERN, Geneva Switzerland (2011).

[34] ATLAS collaboration, *The ATLAS simulation infrastructure*, *Eur. Phys. J.* **C 70** (2010) 823 [arXiv:1005.4568] [INSPIRE].

[35] GEANT4 collaboration, S. Agostinelli et al., *GEANT4: a simulation toolkit*, *Nucl. Instrum. Meth.* **A 506** (2003) 250 [INSPIRE].

[36] ATLAS collaboration, *Muon reconstruction efficiency in reprocessed 2010 LHC proton-proton collision data recorded with the ATLAS detector*, ATLAS-CONF-2011-063, CERN, Geneva Switzerland (2011).

[37] ATLAS collaboration, *A measurement of the muon reconstruction efficiency in 2010 ATLAS data using J/ψ decays*, ATLAS-CONF-2012-125, CERN, Geneva Switzerland (2012).

[38] ATLAS collaboration, *Muon momentum resolution in first pass reconstruction of pp collision data recorded by ATLAS in 2010*, ATLAS-CONF-2011-046, CERN, Geneva Switzerland (2011).

[39] R. Gavin, Y. Li, F. Petriello and S. Quackenbush, *FEWZ 2.0: a code for hadronic Z production at next-to-next-to-leading order*, *Comput. Phys. Commun.* **182** (2011) 2388 [arXiv:1011.3540] [INSPIRE].

[40] R. Gavin, Y. Li, F. Petriello and S. Quackenbush, *W physics at the LHC with FEWZ 2.1*, *Comput. Phys. Commun.* **184** (2013) 208 [arXiv:1201.5896] [INSPIRE].

[41] Y. Li and F. Petriello, *Combining QCD and electroweak corrections to dilepton production in FEWZ*, *Phys. Rev.* **D 86** (2012) 094034 [arXiv:1208.5967] [INSPIRE].

[42] W.F.L. Hollik, *Radiative corrections in the Standard Model and their role for precision tests of the electroweak theory*, *Fortsch. Phys.* **38** (1990) 165 [INSPIRE].

[43] Particle Data Group collaboration, J. Beringer et al., *Review of particle physics (RPP)*, *Phys. Rev.* **D 86** (2012) 010001 [INSPIRE].

[44] D. Bardin et al., *SANC integrator in the progress: QCD and EW contributions*, *JETP Lett.* **96** (2012) 285 [arXiv:1207.4400] [INSPIRE].

[45] A.B. Arbuzov, R.R. Sadykov and Z. Was, *QED bremsstrahlung in decays of electroweak bosons*, *Eur. Phys. J.* **C 73** (2013) 2625 [arXiv:1212.6783] [INSPIRE].

[46] P. Nason, *A new method for combining NLO QCD with shower Monte Carlo algorithms*, *JHEP* **11** (2004) 040 [hep-ph/0409146] [INSPIRE].

[47] S. Frixione, P. Nason and C. Oleari, *Matching NLO QCD computations with parton shower simulations: the POWHEG method*, *JHEP* **11** (2007) 070 [arXiv:0709.2092] [INSPIRE].

[48] S. Alioli, P. Nason, C. Oleari and E. Re, *A general framework for implementing NLO calculations in shower Monte Carlo programs: the POWHEG BOX*, *JHEP* **06** (2010) 043 [arXiv:1002.2581] [INSPIRE].

[49] S. Frixione and G. Ridolfi, *Jet photoproduction at HERA*, *Nucl. Phys.* **B 507** (1997) 315 [hep-ph/9707345] [INSPIRE].

[50] ATLAS collaboration, *A measurement of the ATLAS muon reconstruction and trigger efficiency using J/ψ decays*, ATLAS-CONF-2011-021, CERN, Geneva Switzerland (2011).

[51] G. D'Agostini, *Improved iterative Bayesian unfolding*, arXiv:1010.0632.

JHEP06(2014)112

[52] ATLAS collaboration, *Measurement of angular correlations in Drell-Yan lepton pairs to probe $Z/\gamma^\star$ boson transverse momentum at $\sqrt{s} = 7$ TeV with the ATLAS detector*, *Phys. Lett.* **B 720** (2013) 32 [arXiv:1211.6899] [INSPIRE].

[53] ATLAS collaboration, *Improved luminosity determination in pp collisions at $\sqrt{s} = 7$ TeV using the ATLAS detector at the LHC*, *Eur. Phys. J.* **C 73** (2013) 2518 [arXiv:1302.4393] [INSPIRE].

[54] A. Glazov, *Averaging of DIS cross section data*, *AIP Conf. Proc.* **792** (2005) 237 [INSPIRE].

[55] H1 collaboration, F.D. Aaron et al., *Measurement of the inclusive ep scattering cross section at low Q^2 and x at HERA*, *Eur. Phys. J.* **C 63** (2009) 625 [arXiv:0904.0929] [INSPIRE].

[56] S. Dittmaier and M. Huber, *Radiative corrections to the neutral-current Drell-Yan process in the Standard Model and its minimal supersymmetric extension*, *JHEP* **01** (2010) 060 [arXiv:0911.2329] [INSPIRE].

[57] *Precision analysis of LHC data on neutral and charged current Drell-Yan processes*. work done within CERN-RFBR-Scientific-Cooperation 12-02-91526-CERN_a, CERN, Geneva Switzerland.

[58] A.D. Martin, R.G. Roberts, W.J. Stirling and R.S. Thorne, *Parton distributions incorporating QED contributions*, *Eur. Phys. J.* **C 39** (2005) 155 [hep-ph/0411040] [INSPIRE].

[59] J.M. Campbell and R.K. Ellis, *MCFM for the Tevatron and the LHC*, *Nucl. Phys. Proc. Suppl.* **205-206** (2010) 10 [arXiv:1007.3492] [INSPIRE].

[60] T. Carli et al., *A posteriori inclusion of parton density functions in NLO QCD final-state calculations at hadron colliders: the APPLGRID Project*, *Eur. Phys. J.* **C 66** (2010) 503 [arXiv:0911.2985] [INSPIRE].

[61] H1 collaboration, F.D. Aaron et al., *A precision measurement of the inclusive ep scattering cross section at HERA*, *Eur. Phys. J.* **C 64** (2009) 561 [arXiv:0904.3513] [INSPIRE].

[62] H1 and ZEUS collaborations, F.D. Aaron et al., *Combined measurement and QCD analysis of the inclusive $e^\pm p$ scattering cross sections at HERA*, *JHEP* **01** (2010) 109 [arXiv:0911.0884] [INSPIRE].

[63] H1 collaboration, F.D. Aaron et al., *A precision measurement of the inclusive ep scattering cross section at HERA*, *Eur. Phys. J.* **C 64** (2009) 561 [arXiv:0904.3513] [INSPIRE].

[64] M. Botje, *QCDNUM: fast QCD evolution and convolution*, *Comput. Phys. Commun.* **182** (2011) 490 [arXiv:1005.1481] [INSPIRE].

[65] F. James and M. Roos, *Minuit: a system for function minimization and analysis of the parameter errors and correlations*, *Comput. Phys. Commun.* **10** (1975) 343 [INSPIRE].

[66] R.S. Thorne and R.G. Roberts, *An ordered analysis of heavy flavor production in deep inelastic scattering*, *Phys. Rev.* **D 57** (1998) 6871 [hep-ph/9709442] [INSPIRE].

[67] R.S. Thorne, *A variable-flavor number scheme for NNLO*, *Phys. Rev.* **D 73** (2006) 054019 [CAVENDISH-HEP-2006-01] [hep-ph/0601245] [INSPIRE].

[68] ATLAS collaboration, *Determination of the strange quark density of the proton from ATLAS measurements of the $W \to \ell\nu$ and $Z \to \ell\ell$ cross sections*, *Phys. Rev. Lett.* **109** (2012) 012001 [arXiv:1203.4051] [INSPIRE].

JHEP06(2014)112

The ATLAS collaboration

G. Aad[84], T. Abajyan[21], B. Abbott[112], J. Abdallah[152], S. Abdel Khalek[116], O. Abdinov[11], R. Aben[106], B. Abi[113], M. Abolins[89], O.S. AbouZeid[159], H. Abramowicz[154], H. Abreu[137], Y. Abulaiti[147a,147b], B.S. Acharya[165a,165b,a], L. Adamczyk[38a], D.L. Adams[25], J. Adelman[177], S. Adomeit[99], T. Adye[130], T. Agatonovic-Jovin[13b], J.A. Aguilar-Saavedra[125f,125a], M. Agustoni[17], S.P. Ahlen[22], A. Ahmad[149], F. Ahmadov[64,b], G. Aielli[134a,134b], T.P.A. Åkesson[80], G. Akimoto[156], A.V. Akimov[95], J. Albert[170], S. Albrand[55], M.J. Alconada Verzini[70], M. Aleksa[30], I.N. Aleksandrov[64], C. Alexa[26a], G. Alexander[154], G. Alexandre[49], T. Alexopoulos[10], M. Alhroob[165a,165c], G. Alimonti[90a], L. Alio[84], J. Alison[31], B.M.M. Allbrooke[18], L.J. Allison[71], P.P. Allport[73], S.E. Allwood-Spiers[53], J. Almond[83], A. Aloisio[103a,103b], R. Alon[173], A. Alonso[36], F. Alonso[70], C. Alpigiani[75], A. Altheimer[35], B. Alvarez Gonzalez[89], M.G. Alviggi[103a,103b], K. Amako[65], Y. Amaral Coutinho[24a], C. Amelung[23], D. Amidei[88], V.V. Ammosov[129,*], S.P. Amor Dos Santos[125a,125c], A. Amorim[125a,125b], S. Amoroso[48], N. Amram[154], G. Amundsen[23], C. Anastopoulos[140], L.S. Ancu[17], N. Andari[30], T. Andeen[35], C.F. Anders[58b], G. Anders[30], K.J. Anderson[31], A. Andreazza[90a,90b], V. Andrei[58a], X.S. Anduaga[70], S. Angelidakis[9], P. Anger[44], A. Angerami[35], F. Anghinolfi[30], A.V. Anisenkov[108], N. Anjos[125a], A. Annovi[47], A. Antonaki[9], M. Antonelli[47], A. Antonov[97], J. Antos[145b], F. Anulli[133a], M. Aoki[65], L. Aperio Bella[18], R. Apolle[119,c], G. Arabidze[89], I. Aracena[144], Y. Arai[65], J.P. Araque[125a], A.T.H. Arce[45], J-F. Arguin[94], S. Argyropoulos[42], M. Arik[19a], A.J. Armbruster[30], O. Arnaez[82], V. Arnal[81], O. Arslan[21], A. Artamonov[96], G. Artoni[23], S. Asai[156], N. Asbah[94], A. Ashkenazi[154], S. Ask[28], B. Åsman[147a,147b], L. Asquith[6], K. Assamagan[25], R. Astalos[145a], M. Atkinson[166], N.B. Atlay[142], B. Auerbach[6], E. Auge[116], K. Augsten[127], M. Aurousseau[146b], G. Avolio[30], G. Azuelos[94,d], Y. Azuma[156], M.A. Baak[30], C. Bacci[135a,135b], H. Bachacou[137], K. Bachas[155], M. Backes[30], M. Backhaus[30], J. Backus Mayes[144], E. Badescu[26a], P. Bagiacchi[133a,133b], P. Bagnaia[133a,133b], Y. Bai[33a], D.C. Bailey[159], T. Bain[35], J.T. Baines[130], O.K. Baker[177], S. Baker[77], P. Balek[128], F. Balli[137], E. Banas[39], Sw. Banerjee[174], D. Banfi[30], A. Bangert[151], A.A.E. Bannoura[176], V. Bansal[170], H.S. Bansil[18], L. Barak[173], S.P. Baranov[95], T. Barber[48], E.L. Barberio[87], D. Barberis[50a,50b], M. Barbero[84], T. Barillari[100], M. Barisonzi[176], T. Barklow[144], N. Barlow[28], B.M. Barnett[130], R.M. Barnett[15], Z. Barnovska[5], A. Baroncelli[135a], G. Barone[49], A.J. Barr[119], F. Barreiro[81], J. Barreiro Guimarães da Costa[57], R. Bartoldus[144], A.E. Barton[71], P. Bartos[145a], V. Bartsch[150], A. Bassalat[116], A. Basye[166], R.L. Bates[53], L. Batkova[145a], J.R. Batley[28], M. Battistin[30], F. Bauer[137], H.S. Bawa[144,e], T. Beau[79], P.H. Beauchemin[162], R. Beccherle[123a,123b], P. Bechtle[21], H.P. Beck[17], K. Becker[176], S. Becker[99], M. Beckingham[139], C. Becot[116], A.J. Beddall[19c], A. Beddall[19c], S. Bedikian[177], V.A. Bednyakov[64], C.P. Bee[149], L.J. Beemster[106], T.A. Beermann[176], M. Begel[25], K. Behr[119], C. Belanger-Champagne[86], P.J. Bell[49], W.H. Bell[49], G. Bella[154], L. Bellagamba[20a], A. Bellerive[29], M. Bellomo[85], A. Belloni[57], O.L. Beloborodova[108,f], K. Belotskiy[97], O. Beltramello[30], O. Benary[154], D. Benchekroun[136a], K. Bendtz[147a,147b], N. Benekos[166], Y. Benhammou[154], E. Benhar Noccioli[49], J.A. Benitez Garcia[160b], D.P. Benjamin[45], J.R. Bensinger[23], K. Benslama[131], S. Bentvelsen[106], D. Berge[106], E. Bergeaas Kuutmann[16], N. Berger[5], F. Berghaus[170], E. Berglund[106], J. Beringer[15], C. Bernard[22], P. Bernat[77], C. Bernius[78], F.U. Bernlochner[170], T. Berry[76], P. Berta[128], C. Bertella[84], F. Bertolucci[123a,123b], M.I. Besana[90a], G.J. Besjes[105], O. Bessidskaia[147a,147b], N. Besson[137], C. Betancourt[48], S. Bethke[100], W. Bhimji[46], R.M. Bianchi[124], L. Bianchini[23], M. Bianco[30], O. Biebel[99], S.P. Bieniek[77], K. Bierwagen[54], J. Biesiada[15], M. Biglietti[135a], J. Bilbao De Mendizabal[49], H. Bilokon[47], M. Bindi[54], S. Binet[116], A. Bingul[19c], C. Bini[133a,133b], C.W. Black[151], J.E. Black[144], K.M. Black[22], D. Blackburn[139], R.E. Blair[6], J.-B. Blanchard[137], T. Blazek[145a], I. Bloch[42], C. Blocker[23], W. Blum[82,*], U. Blumenschein[54], G.J. Bobbink[106],

JHEP06(2014)112

V.S. Bobrovnikov[108], S.S. Bocchetta[80], A. Bocci[45], C.R. Boddy[119], M. Boehler[48], J. Boek[176], T.T. Boek[176], J.A. Bogaerts[30], A.G. Bogdanchikov[108], A. Bogouch[91,*], C. Bohm[147a], J. Bohm[126], V. Boisvert[76], T. Bold[38a], V. Boldea[26a], A.S. Boldyrev[98], N.M. Bolnet[137], M. Bomben[79], M. Bona[75], M. Boonekamp[137], A. Borisov[129], G. Borissov[71], M. Borri[83], S. Borroni[42], J. Bortfeldt[99], V. Bortolotto[135a,135b], K. Bos[106], D. Boscherini[20a], M. Bosman[12], H. Boterenbrood[106], J. Boudreau[124], J. Bouffard[2], E.V. Bouhova-Thacker[71], D. Boumediene[34], C. Bourdarios[116], N. Bousson[113], S. Boutouil[136d], A. Boveia[31], J. Boyd[30], I.R. Boyko[64], I. Bozovic-Jelisavcic[13b], J. Bracinik[18], P. Branchini[135a], A. Brandt[8], G. Brandt[15], O. Brandt[58a], U. Bratzler[157], B. Brau[85], J.E. Brau[115], H.M. Braun[176,*], S.F. Brazzale[165a,165c], B. Brelier[159], K. Brendlinger[121], A.J. Brennan[87], R. Brenner[167], S. Bressler[173], K. Bristow[146c], T.M. Bristow[46], D. Britton[53], F.M. Brochu[28], I. Brock[21], R. Brock[89], C. Bromberg[89], J. Bronner[100], G. Brooijmans[35], T. Brooks[76], W.K. Brooks[32b], J. Brosamer[15], E. Brost[115], G. Brown[83], J. Brown[55], P.A. Bruckman de Renstrom[39], D. Bruncko[145b], R. Bruneliere[48], S. Brunet[60], A. Bruni[20a], G. Bruni[20a], M. Bruschi[20a], L. Bryngemark[80], T. Buanes[14], Q. Buat[143], F. Bucci[49], P. Buchholz[142], R.M. Buckingham[119], A.G. Buckley[53], S.I. Buda[26a], I.A. Budagov[64], F. Buehrer[48], L. Bugge[118], M.K. Bugge[118], O. Bulekov[97], A.C. Bundock[73], H. Burckhart[30], S. Burdin[73], B. Burghgrave[107], S. Burke[130], I. Burmeister[43], E. Busato[34], V. Büscher[82], P. Bussey[53], C.P. Buszello[167], B. Butler[57], J.M. Butler[22], A.I. Butt[3], C.M. Buttar[53], J.M. Butterworth[77], P. Butti[106], W. Buttinger[28], A. Buzatu[53], M. Byszewski[10], S. Cabrera Urbán[168], D. Caforio[20a,20b], O. Cakir[4a], P. Calafiura[15], G. Calderini[79], P. Calfayan[99], R. Calkins[107], L.P. Caloba[24a], D. Calvet[34], S. Calvet[34], R. Camacho Toro[49], S. Camarda[42], D. Cameron[118], L.M. Caminada[15], R. Caminal Armadans[12], S. Campana[30], M. Campanelli[77], A. Campoverde[149], V. Canale[103a,103b], A. Canepa[160a], J. Cantero[81], R. Cantrill[76], T. Cao[40], M.D.M. Capeans Garrido[30], I. Caprini[26a], M. Caprini[26a], M. Capua[37a,37b], R. Caputo[82], R. Cardarelli[134a], T. Carli[30], G. Carlino[103a], L. Carminati[90a,90b], S. Caron[105], E. Carquin[32a], G.D. Carrillo-Montoya[146c], A.A. Carter[75], J.R. Carter[28], J. Carvalho[125a,125c], D. Casadei[77], M.P. Casado[12], E. Castaneda-Miranda[146b], A. Castelli[106], V. Castillo Gimenez[168], N.F. Castro[125a], P. Catastini[57], A. Catinaccio[30], J.R. Catmore[71], A. Cattai[30], G. Cattani[134a,134b], S. Caughron[89], V. Cavaliere[166], D. Cavalli[90a], M. Cavalli-Sforza[12], V. Cavasinni[123a,123b], F. Ceradini[135a,135b], B. Cerio[45], K. Cerny[128], A.S. Cerqueira[24b], A. Cerri[150], L. Cerrito[75], F. Cerutti[15], M. Cerv[30], A. Cervelli[17], S.A. Cetin[19b], A. Chafaq[136a], D. Chakraborty[107], I. Chalupkova[128], K. Chan[3], P. Chang[166], B. Chapleau[86], J.D. Chapman[28], D. Charfeddine[116], D.G. Charlton[18], C.C. Chau[159], C.A. Chavez Barajas[150], S. Cheatham[86], A. Chegwidden[89], S. Chekanov[6], S.V. Chekulaev[160a], G.A. Chelkov[64], M.A. Chelstowska[88], C. Chen[63], H. Chen[25], K. Chen[149], L. Chen[33d,g], S. Chen[33c], X. Chen[146c], Y. Chen[35], H.C. Cheng[88], Y. Cheng[31], A. Cheplakov[64], R. Cherkaoui El Moursli[136e], V. Chernyatin[25,*], E. Cheu[7], L. Chevalier[137], V. Chiarella[47], G. Chiefari[103a,103b], J.T. Childers[6], A. Chilingarov[71], G. Chiodini[72a], A.S. Chisholm[18], R.T. Chislett[77], A. Chitan[26a], M.V. Chizhov[64], S. Chouridou[9], B.K.B. Chow[99], I.A. Christidi[77], D. Chromek-Burckhart[30], M.L. Chu[152], J. Chudoba[126], L. Chytka[114], G. Ciapetti[133a,133b], A.K. Ciftci[4a], R. Ciftci[4a], D. Cinca[62], V. Cindro[74], A. Ciocio[15], P. Cirkovic[13b], Z.H. Citron[173], M. Citterio[90a], M. Ciubancan[26a], A. Clark[49], P.J. Clark[46], R.N. Clarke[15], W. Cleland[124], J.C. Clemens[84], B. Clement[55], C. Clement[147a,147b], Y. Coadou[84], M. Cobal[165a,165c], A. Coccaro[139], J. Cochran[63], L. Coffey[23], J.G. Cogan[144], J. Coggeshall[166], B. Cole[35], S. Cole[107], A.P. Colijn[106], C. Collins-Tooth[53], J. Collot[55], T. Colombo[58c], G. Colon[85], G. Compostella[100], P. Conde Muiño[125a,125b], E. Coniavitis[167], M.C. Conidi[12], S.H. Connell[146b], I.A. Connelly[76], S.M. Consonni[90a,90b], V. Consorti[48], S. Constantinescu[26a], C. Conta[120a,120b], G. Conti[57], F. Conventi[103a,h], M. Cooke[15], B.D. Cooper[77], A.M. Cooper-Sarkar[119], N.J. Cooper-Smith[76], K. Copic[15], T. Cornelissen[176], M. Corradi[20a], F. Corriveau[86,i],

JHEP06(2014)112

A. Corso-Radu[164], A. Cortes-Gonzalez[12], G. Cortiana[100], G. Costa[90a], M.J. Costa[168], D. Costanzo[140], D. Côté[8], G. Cottin[28], G. Cowan[76], B.E. Cox[83], K. Cranmer[109], G. Cree[29], S. Crépé-Renaudin[55], F. Crescioli[79], M. Crispin Ortuzar[119], M. Cristinziani[21], G. Crosetti[37a,37b], C.-M. Cuciuc[26a], C. Cuenca Almenar[177], T. Cuhadar Donszelmann[140], J. Cummings[177], M. Curatolo[47], C. Cuthbert[151], H. Czirr[142], P. Czodrowski[3], Z. Czyczula[177], S. D'Auria[53], M. D'Onofrio[73], M.J. Da Cunha Sargedas De Sousa[125a,125b], C. Da Via[83], W. Dabrowski[38a], A. Dafinca[119], T. Dai[88], O. Dale[14], F. Dallaire[94], C. Dallapiccola[85], M. Dam[36], A.C. Daniells[18], M. Dano Hoffmann[137], V. Dao[105], G. Darbo[50a], G.L. Darlea[26c], S. Darmora[8], J.A. Dassoulas[42], W. Davey[21], C. David[170], T. Davidek[128], E. Davies[119,c], M. Davies[94], O. Davignon[79], A.R. Davison[77], P. Davison[77], Y. Davygora[58a], E. Dawe[143], I. Dawson[140], R.K. Daya-Ishmukhametova[23], K. De[8], R. de Asmundis[103a], S. De Castro[20a,20b], S. De Cecco[79], J. de Graat[99], N. De Groot[105], P. de Jong[106], C. De La Taille[116], H. De la Torre[81], F. De Lorenzi[63], L. De Nooij[106], D. De Pedis[133a], A. De Salvo[133a], U. De Sanctis[165a,165c], A. De Santo[150], J.B. De Vivie De Regie[116], G. De Zorzi[133a,133b], W.J. Dearnaley[71], R. Debbe[25], C. Debenedetti[46], B. Dechenaux[55], D.V. Dedovich[64], J. Degenhardt[121], I. Deigaard[106], J. Del Peso[81], T. Del Prete[123a,123b], F. Deliot[137], C.M. Delitzsch[49], M. Deliyergiyev[74], A. Dell'Acqua[30], L. Dell'Asta[22], M. Dell'Orso[123a,123b], M. Della Pietra[103a,h], D. della Volpe[49], M. Delmastro[5], P.A. Delsart[55], C. Deluca[106], S. Demers[177], M. Demichev[64], A. Demilly[79], S.P. Denisov[129], D. Derendarz[39], J.E. Derkaoui[136d], F. Derue[79], P. Dervan[73], K. Desch[21], C. Deterre[42], P.O. Deviveiros[106], A. Dewhurst[130], S. Dhaliwal[106], A. Di Ciaccio[134a,134b], L. Di Ciaccio[5], A. Di Domenico[133a,133b], C. Di Donato[103a,103b], A. Di Girolamo[30], B. Di Girolamo[30], A. Di Mattia[153], B. Di Micco[135a,135b], R. Di Nardo[47], A. Di Simone[48], R. Di Sipio[20a,20b], D. Di Valentino[29], M.A. Diaz[32a], E.B. Diehl[88], J. Dietrich[42], T.A. Dietzsch[58a], S. Diglio[87], A. Dimitrievska[13a], J. Dingfelder[21], C. Dionisi[133a,133b], P. Dita[26a], S. Dita[26a], F. Dittus[30], F. Djama[84], T. Djobava[51b], M.A.B. do Vale[24c], A. Do Valle Wemans[125a,125g], T.K.O. Doan[5], D. Dobos[30], E. Dobson[77], C. Doglioni[49], T. Doherty[53], T. Dohmae[156], J. Dolejsi[128], Z. Dolezal[128], B.A. Dolgoshein[97,*], M. Donadelli[24d], S. Donati[123a,123b], P. Dondero[120a,120b], J. Donini[34], J. Dopke[30], A. Doria[103a], A. Dos Anjos[174], M.T. Dova[70], A.T. Doyle[53], M. Dris[10], J. Dubbert[88], S. Dube[15], E. Dubreuil[34], E. Duchovni[173], G. Duckeck[99], O.A. Ducu[26a], D. Duda[176], A. Dudarev[30], F. Dudziak[63], L. Duflot[116], L. Duguid[76], M. Dührssen[30], M. Dunford[58a], H. Duran Yildiz[4a], M. Düren[52], A. Durglishvili[51b], M. Dwuznik[38a], M. Dyndal[38a], J. Ebke[99], W. Edson[2], N.C. Edwards[46], W. Ehrenfeld[21], T. Eifert[144], G. Eigen[14], K. Einsweiler[15], T. Ekelof[167], M. El Kacimi[136c], M. Ellert[167], S. Elles[5], F. Ellinghaus[82], N. Ellis[30], J. Elmsheuser[99], M. Elsing[30], D. Emeliyanov[130], Y. Enari[156], O.C. Endner[82], M. Endo[117], R. Engelmann[149], J. Erdmann[177], A. Ereditato[17], D. Eriksson[147a], G. Ernis[176], J. Ernst[2], M. Ernst[25], J. Ernwein[137], D. Errede[166], S. Errede[166], E. Ertel[82], M. Escalier[116], H. Esch[43], C. Escobar[124], B. Esposito[47], A.I. Etienvre[137], E. Etzion[154], H. Evans[60], L. Fabbri[20a,20b], G. Facini[30], R.M. Fakhrutdinov[129], S. Falciano[133a], Y. Fang[33a], M. Fanti[90a,90b], A. Farbin[8], A. Farilla[135a], T. Farooque[12], S. Farrell[164], S.M. Farrington[171], P. Farthouat[30], F. Fassi[168], P. Fassnacht[30], D. Fassouliotis[9], A. Favareto[50a,50b], L. Fayard[116], P. Federic[145a], O.L. Fedin[122], W. Fedorko[169], M. Fehling-Kaschek[48], S. Feigl[30], L. Feligioni[84], C. Feng[33d], E.J. Feng[6], H. Feng[88], A.B. Fenyuk[129], S. Fernandez Perez[30], S. Ferrag[53], J. Ferrando[53], V. Ferrara[42], A. Ferrari[167], P. Ferrari[106], R. Ferrari[120a], D.E. Ferreira de Lima[53], A. Ferrer[168], D. Ferrere[49], C. Ferretti[88], A. Ferretto Parodi[50a,50b], M. Fiascaris[31], F. Fiedler[82], A. Filipčič[74], M. Filipuzzi[42], F. Filthaut[105], M. Fincke-Keeler[170], K.D. Finelli[151], M.C.N. Fiolhais[125a,125c], L. Fiorini[168], A. Firan[40], J. Fischer[176], M.J. Fisher[110], W.C. Fisher[89], E.A. Fitzgerald[23], M. Flechl[48], I. Fleck[142], P. Fleischmann[175], S. Fleischmann[176], G.T. Fletcher[140], G. Fletcher[75], T. Flick[176], A. Floderus[80], L.R. Flores Castillo[174], A.C. Florez Bustos[160b], M.J. Flowerdew[100],

JHEP06(2014)112

A. Formica[137], A. Forti[83], D. Fortin[160a], D. Fournier[116], H. Fox[71], S. Fracchia[12], P. Francavilla[79], M. Franchini[20a,20b], S. Franchino[30], D. Francis[30], M. Franklin[57], S. Franz[61], M. Fraternali[120a,120b], S.T. French[28], C. Friedrich[42], F. Friedrich[44], D. Froidevaux[30], J.A. Frost[28], C. Fukunaga[157], E. Fullana Torregrosa[82], B.G. Fulsom[144], J. Fuster[168], C. Gabaldon[55], O. Gabizon[173], A. Gabrielli[20a,20b], A. Gabrielli[133a,133b], S. Gadatsch[106], S. Gadomski[49], G. Gagliardi[50a,50b], P. Gagnon[60], C. Galea[105], B. Galhardo[125a,125c], E.J. Gallas[119], V. Gallo[17], B.J. Gallop[130], P. Gallus[127], G. Galster[36], K.K. Gan[110], R.P. Gandrajula[62], J. Gao[33b,g], Y.S. Gao[144,e], F.M. Garay Walls[46], F. Garberson[177], C. García[168], J.E. García Navarro[168], M. Garcia-Sciveres[15], R.W. Gardner[31], N. Garelli[144], V. Garonne[30], C. Gatti[47], G. Gaudio[120a], B. Gaur[142], L. Gauthier[94], P. Gauzzi[133a,133b], I.L. Gavrilenko[95], C. Gay[169], G. Gaycken[21], E.N. Gazis[10], P. Ge[33d], Z. Gecse[169], C.N.P. Gee[130], D.A.A. Geerts[106], Ch. Geich-Gimbel[21], K. Gellerstedt[147a,147b], C. Gemme[50a], A. Gemmell[53], M.H. Genest[55], S. Gentile[133a,133b], M. George[54], S. George[76], D. Gerbaudo[164], A. Gershon[154], H. Ghazlane[136b], N. Ghodbane[34], B. Giacobbe[20a], S. Giagu[133a,133b], V. Giangiobbe[12], P. Giannetti[123a,123b], F. Gianotti[30], B. Gibbard[25], S.M. Gibson[76], M. Gilchriese[15], T.P.S. Gillam[28], D. Gillberg[30], G. Gilles[34], D.M. Gingrich[3,d], N. Giokaris[9], M.P. Giordani[165a,165c], R. Giordano[103a,103b], F.M. Giorgi[16], P.F. Giraud[137], D. Giugni[90a], C. Giuliani[48], M. Giulini[58b], B.K. Gjelsten[118], I. Gkialas[155,j], L.K. Gladilin[98], C. Glasman[81], J. Glatzer[30], P.C.F. Glaysher[46], A. Glazov[42], G.L. Glonti[64], M. Goblirsch-Kolb[100], J.R. Goddard[75], J. Godfrey[143], J. Godlewski[30], C. Goeringer[82], S. Goldfarb[88], T. Golling[177], D. Golubkov[129], A. Gomes[125a,125b,125d], L.S. Gomez Fajardo[42], R. Gonçalo[125a], J. Goncalves Pinto Firmino Da Costa[42], L. Gonella[21], S. González de la Hoz[168], G. Gonzalez Parra[12], M.L. Gonzalez Silva[27], S. Gonzalez-Sevilla[49], L. Goossens[30], P.A. Gorbounov[96], H.A. Gordon[25], I. Gorelov[104], G. Gorfine[176], B. Gorini[30], E. Gorini[72a,72b], A. Gorišek[74], E. Gornicki[39], A.T. Goshaw[6], C. Gössling[43], M.I. Gostkin[64], M. Gouighri[136a], D. Goujdami[136c], M.P. Goulette[49], A.G. Goussiou[139], C. Goy[5], S. Gozpinar[23], H.M.X. Grabas[137], L. Graber[54], I. Grabowska-Bold[38a], P. Grafström[20a,20b], K-J. Grahn[42], J. Gramling[49], E. Gramstad[118], F. Grancagnolo[72a], S. Grancagnolo[16], V. Grassi[149], V. Gratchev[122], H.M. Gray[30], E. Graziani[135a], O.G. Grebenyuk[122], Z.D. Greenwood[78,k], K. Gregersen[36], I.M. Gregor[42], P. Grenier[144], J. Griffiths[8], N. Grigalashvili[64], A.A. Grillo[138], K. Grimm[71], S. Grinstein[12,l], Ph. Gris[34], Y.V. Grishkevich[98], J.-F. Grivaz[116], J.P. Grohs[44], A. Grohsjean[42], E. Gross[173], J. Grosse-Knetter[54], G.C. Grossi[134a,134b], J. Groth-Jensen[173], Z.J. Grout[150], K. Grybel[142], L. Guan[33b], F. Guescini[49], D. Guest[177], O. Gueta[154], C. Guicheney[34], E. Guido[50a,50b], T. Guillemin[116], S. Guindon[2], U. Gul[53], C. Gumpert[44], J. Gunther[127], J. Guo[35], S. Gupta[119], P. Gutierrez[112], N.G. Gutierrez Ortiz[53], C. Gutschow[77], N. Guttman[154], C. Guyot[137], C. Gwenlan[119], C.B. Gwilliam[73], A. Haas[109], C. Haber[15], H.K. Hadavand[8], N. Haddad[136e], P. Haefner[21], S. Hageboeck[21], Z. Hajduk[39], H. Hakobyan[178], M. Haleem[42], D. Hall[119], G. Halladjian[89], K. Hamacher[176], P. Hamal[114], K. Hamano[87], M. Hamer[54], A. Hamilton[146a], S. Hamilton[162], P.G. Hamnett[42], L. Han[33b], K. Hanagaki[117], K. Hanawa[156], M. Hance[15], P. Hanke[58a], J.R. Hansen[36], J.B. Hansen[36], J.D. Hansen[36], P.H. Hansen[36], K. Hara[161], A.S. Hard[174], T. Harenberg[176], S. Harkusha[91], D. Harper[88], R.D. Harrington[46], O.M. Harris[139], P.F. Harrison[171], F. Hartjes[106], S. Hasegawa[102], Y. Hasegawa[141], A. Hasib[112], S. Hassani[137], S. Haug[17], M. Hauschild[30], R. Hauser[89], M. Havranek[126], C.M. Hawkes[18], R.J. Hawkings[30], A.D. Hawkins[80], T. Hayashi[161], D. Hayden[89], C.P. Hays[119], H.S. Hayward[73], S.J. Haywood[130], S.J. Head[18], T. Heck[82], V. Hedberg[80], L. Heelan[8], S. Heim[121], T. Heim[176], B. Heinemann[15], L. Heinrich[109], S. Heisterkamp[36], J. Hejbal[126], L. Helary[22], C. Heller[99], M. Heller[30], S. Hellman[147a,147b], D. Hellmich[21], C. Helsens[30], J. Henderson[119], R.C.W. Henderson[71], C. Hengler[42], A. Henrichs[177], A.M. Henriques Correia[30], S. Henrot-Versille[116], C. Hensel[54], G.H. Herbert[16], Y. Hernández Jiménez[168],

JHEP06(2014)112

R. Herrberg-Schubert[16], G. Herten[48], R. Hertenberger[99], L. Hervas[30], G.G. Hesketh[77], N.P. Hessey[106], R. Hickling[75], E. Higón-Rodriguez[168], J.C. Hill[28], K.H. Hiller[42], S. Hillert[21], S.J. Hillier[18], I. Hinchliffe[15], E. Hines[121], M. Hirose[117], D. Hirschbuehl[176], J. Hobbs[149], N. Hod[106], M.C. Hodgkinson[140], P. Hodgson[140], A. Hoecker[30], M.R. Hoeferkamp[104], J. Hoffman[40], D. Hoffmann[84], J.I. Hofmann[58a], M. Hohlfeld[82], T.R. Holmes[15], T.M. Hong[121], L. Hooft van Huysduynen[109], J-Y. Hostachy[55], S. Hou[152], A. Hoummada[136a], J. Howard[119], J. Howarth[42], M. Hrabovsky[114], I. Hristova[16], J. Hrivnac[116], T. Hryn'ova[5], P.J. Hsu[82], S.-C. Hsu[139], D. Hu[35], X. Hu[25], Y. Huang[42], Z. Hubacek[30], F. Hubaut[84], F. Huegging[21], T.B. Huffman[119], E.W. Hughes[35], G. Hughes[71], M. Huhtinen[30], T.A. Hülsing[82], M. Hurwitz[15], N. Huseynov[64,b], J. Huston[89], J. Huth[57], G. Iacobucci[49], G. Iakovidis[10], I. Ibragimov[142], L. Iconomidou-Fayard[116], J. Idarraga[116], E. Ideal[177], P. Iengo[103a], O. Igonkina[106], T. Iizawa[172], Y. Ikegami[65], K. Ikematsu[142], M. Ikeno[65], D. Iliadis[155], N. Ilic[159], Y. Inamaru[66], T. Ince[100], P. Ioannou[9], M. Iodice[135a], K. Iordanidou[9], V. Ippolito[57], A. Irles Quiles[168], C. Isaksson[167], M. Ishino[67], M. Ishitsuka[158], R. Ishmukhametov[110], C. Issever[119], S. Istin[19a], J.M. Iturbe Ponce[83], A.V. Ivashin[129], W. Iwanski[39], H. Iwasaki[65], J.M. Izen[41], V. Izzo[103a], B. Jackson[121], J.N. Jackson[73], M. Jackson[73], P. Jackson[1], M.R. Jaekel[30], V. Jain[2], K. Jakobs[48], S. Jakobsen[36], T. Jakoubek[126], J. Jakubek[127], D.O. Jamin[152], D.K. Jana[78], E. Jansen[77], H. Jansen[30], J. Janssen[21], M. Janus[171], G. Jarlskog[80], T. Javůrek[48], L. Jeanty[15], G.-Y. Jeng[151], D. Jennens[87], P. Jenni[48,m], J. Jentzsch[43], C. Jeske[171], S. Jézéquel[5], H. Ji[174], W. Ji[82], J. Jia[149], Y. Jiang[33b], M. Jimenez Belenguer[42], S. Jin[33a], A. Jinaru[26a], O. Jinnouchi[158], M.D. Joergensen[36], K.E. Johansson[147a], P. Johansson[140], K.A. Johns[7], K. Jon-And[147a,147b], G. Jones[171], R.W.L. Jones[71], T.J. Jones[73], J. Jongmanns[58a], P.M. Jorge[125a,125b], K.D. Joshi[83], J. Jovicevic[148], X. Ju[174], C.A. Jung[43], R.M. Jungst[30], P. Jussel[61], A. Juste Rozas[12,l], M. Kaci[168], A. Kaczmarska[39], M. Kado[116], H. Kagan[110], M. Kagan[144], E. Kajomovitz[45], S. Kama[40], N. Kanaya[156], M. Kaneda[30], S. Kaneti[28], T. Kanno[158], V.A. Kantserov[97], J. Kanzaki[65], B. Kaplan[109], A. Kapliy[31], D. Kar[53], K. Karakostas[10], N. Karastathis[10], M. Karnevskiy[82], S.N. Karpov[64], K. Karthik[109], V. Kartvelishvili[71], A.N. Karyukhin[129], L. Kashif[174], G. Kasieczka[58b], R.D. Kass[110], A. Kastanas[14], Y. Kataoka[156], A. Katre[49], J. Katzy[42], V. Kaushik[7], K. Kawagoe[69], T. Kawamoto[156], G. Kawamura[54], S. Kazama[156], V.F. Kazanin[108], M.Y. Kazarinov[64], R. Keeler[170], P.T. Keener[121], R. Kehoe[40], M. Keil[54], J.S. Keller[42], H. Keoshkerian[5], O. Kepka[126], B.P. Kerševan[74], S. Kersten[176], K. Kessoku[156], J. Keung[159], F. Khalil-zada[11], H. Khandanyan[147a,147b], A. Khanov[113], A. Khodinov[97], A. Khomich[58a], T.J. Khoo[28], G. Khoriauli[21], A. Khoroshilov[176], V. Khovanskiy[96], E. Khramov[64], J. Khubua[51b], H.Y. Kim[8], H. Kim[147a,147b], S.H. Kim[161], N. Kimura[172], O. Kind[16], B.T. King[73], M. King[168], R.S.B. King[119], S.B. King[169], J. Kirk[130], A.E. Kiryunin[100], T. Kishimoto[66], D. Kisielewska[38a], F. Kiss[48], T. Kitamura[66], T. Kittelmann[124], K. Kiuchi[161], E. Kladiva[145b], M. Klein[73], U. Klein[73], K. Kleinknecht[82], P. Klimek[147a,147b], A. Klimentov[25], R. Klingenberg[43], J.A. Klinger[83], E.B. Klinkby[36], T. Klioutchnikova[30], P.F. Klok[105], E.-E. Kluge[58a], P. Kluit[106], S. Kluth[100], E. Kneringer[61], E.B.F.G. Knoops[84], A. Knue[53], T. Kobayashi[156], M. Kobel[44], M. Kocian[144], P. Kodys[128], P. Koevesarki[21], T. Koffas[29], E. Koffeman[106], L.A. Kogan[119], S. Kohlmann[176], Z. Kohout[127], T. Kohriki[65], T. Koi[144], H. Kolanoski[16], I. Koletsou[5], J. Koll[89], A.A. Komar[95,*], Y. Komori[156], T. Kondo[65], N. Kondrashova[42], K. Köneke[48], A.C. König[105], S. König[82], T. Kono[65,n], R. Konoplich[109,o], N. Konstantinidis[77], R. Kopeliansky[153], S. Koperny[38a], L. Köpke[82], A.K. Kopp[48], K. Korcyl[39], K. Kordas[155], A. Korn[77], A.A. Korol[108], I. Korolkov[12], E.V. Korolkova[140], V.A. Korotkov[129], O. Kortner[100], S. Kortner[100], V.V. Kostyukhin[21], S. Kotov[100], V.M. Kotov[64], A. Kotwal[45], C. Kourkoumelis[9], V. Kouskoura[155], A. Koutsman[160a], R. Kowalewski[170], T.Z. Kowalski[38a], W. Kozanecki[137], A.S. Kozhin[129], V. Kral[127], V.A. Kramarenko[98], G. Kramberger[74], D. Krasnopevtsev[97], M.W. Krasny[79], A. Krasznahorkay[30],

JHEP06(2014)112

J.K. Kraus[21], A. Kravchenko[25], S. Kreiss[109], M. Kretz[58c], J. Kretzschmar[73], K. Kreutzfeldt[52], P. Krieger[159], K. Kroeninger[54], H. Kroha[100], J. Kroll[121], J. Kroseberg[21], J. Krstic[13a], U. Kruchonak[64], H. Krüger[21], T. Kruker[17], N. Krumnack[63], Z.V. Krumshteyn[64], A. Kruse[174], M.C. Kruse[45], M. Kruskal[22], T. Kubota[87], S. Kuday[4a], S. Kuehn[48], A. Kugel[58c], A. Kuhl[138], T. Kuhl[42], V. Kukhtin[64], Y. Kulchitsky[91], S. Kuleshov[32b], M. Kuna[133a,133b], J. Kunkle[121], A. Kupco[126], H. Kurashige[66], Y.A. Kurochkin[91], R. Kurumida[66], V. Kus[126], E.S. Kuwertz[148], M. Kuze[158], J. Kvita[143], T. Kwan[170], A. La Rosa[49], L. La Rotonda[37a,37b], L. Labarga[81], C. Lacasta[168], F. Lacava[133a,133b], J. Lacey[29], H. Lacker[16], D. Lacour[79], V.R. Lacuesta[168], E. Ladygin[64], R. Lafaye[5], B. Laforge[79], T. Lagouri[177], S. Lai[48], H. Laier[58a], L. Lambourne[77], S. Lammers[60], C.L. Lampen[7], W. Lampl[7], E. Lançon[137], U. Landgraf[48], M.P.J. Landon[75], V.S. Lang[58a], C. Lange[42], A.J. Lankford[164], F. Lanni[25], K. Lantzsch[30], A. Lanza[120a], S. Laplace[79], C. Lapoire[21], J.F. Laporte[137], T. Lari[90a], M. Lassnig[30], P. Laurelli[47], V. Lavorini[37a,37b], W. Lavrijsen[15], A.T. Law[138], P. Laycock[73], B.T. Le[55], O. Le Dortz[79], E. Le Guirriec[84], E. Le Menedeu[12], T. LeCompte[6], F. Ledroit-Guillon[55], C.A. Lee[152], H. Lee[106], J.S.H. Lee[117], S.C. Lee[152], L. Lee[177], G. Lefebvre[79], M. Lefebvre[170], F. Legger[99], C. Leggett[15], A. Lehan[73], M. Lehmacher[21], G. Lehmann Miotto[30], X. Lei[7], A.G. Leister[177], M.A.L. Leite[24d], R. Leitner[128], D. Lellouch[173], B. Lemmer[54], K.J.C. Leney[77], T. Lenz[106], G. Lenzen[176], B. Lenzi[30], R. Leone[7], K. Leonhardt[44], S. Leontsinis[10], C. Leroy[94], C.G. Lester[28], C.M. Lester[121], J. Levêque[5], D. Levin[88], L.J. Levinson[173], M. Levy[18], A. Lewis[119], G.H. Lewis[109], A.M. Leyko[21], M. Leyton[41], B. Li[33b,p], B. Li[84], H. Li[149], H.L. Li[31], S. Li[45], X. Li[88], Y. Li[116,q], Z. Liang[119,r], H. Liao[34], B. Liberti[134a], P. Lichard[30], K. Lie[166], J. Liebal[21], W. Liebig[14], C. Limbach[21], A. Limosani[87], M. Limper[62], S.C. Lin[152,s], F. Linde[106], B.E. Lindquist[149], J.T. Linnemann[89], E. Lipeles[121], A. Lipniacka[14], M. Lisovyi[42], T.M. Liss[166], D. Lissauer[25], A. Lister[169], A.M. Litke[138], B. Liu[152], D. Liu[152], J.B. Liu[33b], K. Liu[33b,t], L. Liu[88], M. Liu[45], M. Liu[33b], Y. Liu[33b], M. Livan[120a,120b], S.S.A. Livermore[119], A. Lleres[55], J. Llorente Merino[81], S.L. Lloyd[75], F. Lo Sterzo[152], E. Lobodzinska[42], P. Loch[7], W.S. Lockman[138], T. Loddenkoetter[21], F.K. Loebinger[83], A.E. Loevschall-Jensen[36], A. Loginov[177], C.W. Loh[169], T. Lohse[16], K. Lohwasser[48], M. Lokajicek[126], V.P. Lombardo[5], J.D. Long[88], R.E. Long[71], L. Lopes[125a], D. Lopez Mateos[57], B. Lopez Paredes[140], J. Lorenz[99], N. Lorenzo Martinez[60], M. Losada[163], P. Loscutoff[15], X. Lou[41], A. Lounis[116], J. Love[6], P.A. Love[71], A.J. Lowe[144,e], F. Lu[33a], H.J. Lubatti[139], C. Luci[133a,133b], A. Lucotte[55], F. Luehring[60], W. Lukas[61], L. Luminari[133a], O. Lundberg[147a,147b], B. Lund-Jensen[148], M. Lungwitz[82], D. Lynn[25], R. Lysak[126], E. Lytken[80], H. Ma[25], L.L. Ma[33d], G. Maccarrone[47], A. Macchiolo[100], B. Maček[74], J. Machado Miguens[125a,125b], D. Macina[30], D. Madaffari[84], R. Madar[48], H.J. Maddocks[71], W.F. Mader[44], A. Madsen[167], M. Maeno[8], T. Maeno[25], E. Magradze[54], K. Mahboubi[48], J. Mahlstedt[106], S. Mahmoud[73], C. Maiani[137], C. Maidantchik[24a], A. Maio[125a,125b,125d], S. Majewski[115], Y. Makida[65], N. Makovec[116], P. Mal[137,u], B. Malaescu[79], Pa. Malecki[39], V.P. Maleev[122], F. Malek[55], U. Mallik[62], D. Malon[6], C. Malone[144], S. Maltezos[10], V.M. Malyshev[108], S. Malyukov[30], J. Mamuzic[13b], B. Mandelli[30], L. Mandelli[90a], I. Mandić[74], R. Mandrysch[62], J. Maneira[125a,125b], A. Manfredini[100], L. Manhaes de Andrade Filho[24b], J.A. Manjarres Ramos[160b], A. Mann[99], P.M. Manning[138], A. Manousakis-Katsikakis[9], B. Mansoulie[137], R. Mantifel[86], L. Mapelli[30], L. March[168], J.F. Marchand[29], G. Marchiori[79], M. Marcisovsky[126], C.P. Marino[170], C.N. Marques[125a], F. Marroquim[24a], S.P. Marsden[83], Z. Marshall[15], L.F. Marti[17], S. Marti-Garcia[168], B. Martin[30], B. Martin[89], J.P. Martin[94], T.A. Martin[171], V.J. Martin[46], B. Martin dit Latour[14], H. Martinez[137], M. Martinez[12,l], S. Martin-Haugh[130], A.C. Martyniuk[77], M. Marx[139], F. Marzano[133a], A. Marzin[30], L. Masetti[82], T. Mashimo[156], R. Mashinistov[95], J. Masik[83], A.L. Maslennikov[108], I. Massa[20a,20b], N. Massol[5], P. Mastrandrea[149], A. Mastroberardino[37a,37b], T. Masubuchi[156], P. Matricon[116], H. Matsunaga[156], T. Matsushita[66], P. Mättig[176], S. Mättig[42],

JHEP06(2014)112

J. Mattmann[82], J. Maurer[26a], S.J. Maxfield[73], D.A. Maximov[108,f], R. Mazini[152], L. Mazzaferro[134a,134b], G. Mc Goldrick[159], S.P. Mc Kee[88], A. McCarn[88], R.L. McCarthy[149], T.G. McCarthy[29], N.A. McCubbin[130], K.W. McFarlane[56,*], J.A. Mcfayden[77], G. Mchedlidze[54], T. Mclaughlan[18], S.J. McMahon[130], R.A. McPherson[170,i], A. Meade[85], J. Mechnich[106], M. Medinnis[42], S. Meehan[31], R. Meera-Lebbai[112], S. Mehlhase[36], A. Mehta[73], K. Meier[58a], C. Meineck[99], B. Meirose[80], C. Melachrinos[31], B.R. Mellado Garcia[146c], F. Meloni[90a,90b], A. Mengarelli[20a,20b], S. Menke[100], E. Meoni[162], K.M. Mercurio[57], S. Mergelmeyer[21], N. Meric[137], P. Mermod[49], L. Merola[103a,103b], C. Meroni[90a], F.S. Merritt[31], H. Merritt[110], A. Messina[30,v], J. Metcalfe[25], A.S. Mete[164], C. Meyer[82], C. Meyer[31], J-P. Meyer[137], J. Meyer[30], R.P. Middleton[130], S. Migas[73], L. Mijović[137], G. Mikenberg[173], M. Mikestikova[126], M. Mikuž[74], D.W. Miller[31], C. Mills[46], A. Milov[173], D.A. Milstead[147a,147b], D. Milstein[173], A.A. Minaenko[129], M. Miñano Moya[168], I.A. Minashvili[64], A.I. Mincer[109], B. Mindur[38a], M. Mineev[64], Y. Ming[174], L.M. Mir[12], G. Mirabelli[133a], T. Mitani[172], J. Mitrevski[99], V.A. Mitsou[168], S. Mitsui[65], A. Miucci[49], P.S. Miyagawa[140], J.U. Mjörnmark[80], T. Moa[147a,147b], K. Mochizuki[84], V. Moeller[28], S. Mohapatra[35], W. Mohr[48], S. Molander[147a,147b], R. Moles-Valls[168], K. Mönig[42], C. Monini[55], J. Monk[36], E. Monnier[84], J. Montejo Berlingen[12], F. Monticelli[70], S. Monzani[133a,133b], R.W. Moore[3], A. Moraes[53], N. Morange[62], J. Morel[54], D. Moreno[82], M. Moreno Llácer[54], P. Morettini[50a], M. Morgenstern[44], M. Morii[57], S. Moritz[82], A.K. Morley[148], G. Mornacchi[30], J.D. Morris[75], L. Morvaj[102], H.G. Moser[100], M. Mosidze[51b], J. Moss[110], R. Mount[144], E. Mountricha[25], S.V. Mouraviev[95,*], E.J.W. Moyse[85], S.G. Muanza[84], R.D. Mudd[18], F. Mueller[58a], J. Mueller[124], K. Mueller[21], T. Mueller[28], T. Mueller[82], D. Muenstermann[49], Y. Munwes[154], J.A. Murillo Quijada[18], W.J. Murray[171,130], H. Musheghyan[54], E. Musto[153], A.G. Myagkov[129,w], M. Myska[126], O. Nackenhorst[54], J. Nadal[54], K. Nagai[61], R. Nagai[158], Y. Nagai[84], K. Nagano[65], A. Nagarkar[110], Y. Nagasaka[59], M. Nagel[100], A.M. Nairz[30], Y. Nakahama[30], K. Nakamura[65], T. Nakamura[156], I. Nakano[111], H. Namasivayam[41], G. Nanava[21], R. Narayan[58b], T. Nattermann[21], T. Naumann[42], G. Navarro[163], R. Nayyar[7], H.A. Neal[88], P.Yu. Nechaeva[95], T.J. Neep[83], A. Negri[120a,120b], G. Negri[30], M. Negrini[20a], S. Nektarijevic[49], A. Nelson[164], T.K. Nelson[144], S. Nemecek[126], P. Nemethy[109], A.A. Nepomuceno[24a], M. Nessi[30,x], M.S. Neubauer[166], M. Neumann[176], R.M. Neves[109], P. Nevski[25], F.M. Newcomer[121], P.R. Newman[18], D.H. Nguyen[6], R.B. Nickerson[119], R. Nicolaidou[137], B. Nicquevert[30], J. Nielsen[138], N. Nikiforou[35], A. Nikiforov[16], V. Nikolaenko[129,w], I. Nikolic-Audit[79], K. Nikolics[49], K. Nikolopoulos[18], P. Nilsson[8], Y. Ninomiya[156], A. Nisati[133a], R. Nisius[100], T. Nobe[158], L. Nodulman[6], M. Nomachi[117], I. Nomidis[155], S. Norberg[112], M. Nordberg[30], J. Novakova[128], S. Nowak[100], M. Nozaki[65], L. Nozka[114], K. Ntekas[10], G. Nunes Hanninger[87], T. Nunnemann[99], E. Nurse[77], F. Nuti[87], B.J. O'Brien[46], F. O'grady[7], D.C. O'Neil[143], V. O'Shea[53], F.G. Oakham[29,d], H. Oberlack[100], T. Obermann[21], J. Ocariz[79], A. Ochi[66], M.I. Ochoa[77], S. Oda[69], S. Odaka[65], H. Ogren[60], A. Oh[83], S.H. Oh[45], C.C. Ohm[30], H. Ohman[167], T. Ohshima[102], W. Okamura[117], H. Okawa[25], Y. Okumura[31], T. Okuyama[156], A. Olariu[26a], A.G. Olchevski[64], S.A. Olivares Pino[46], D. Oliveira Damazio[25], E. Oliver Garcia[168], D. Olivito[121], A. Olszewski[39], J. Olszowska[39], A. Onofre[125a,125e], P.U.E. Onyisi[31,y], C.J. Oram[160a], M.J. Oreglia[31], Y. Oren[154], D. Orestano[135a,135b], N. Orlando[72a,72b], C. Oropeza Barrera[53], R.S. Orr[159], B. Osculati[50a,50b], R. Ospanov[121], G. Otero y Garzon[27], H. Otono[69], M. Ouchrif[136d], E.A. Ouellette[170], F. Ould-Saada[118], A. Ouraou[137], K.P. Oussoren[106], Q. Ouyang[33a], A. Ovcharova[15], M. Owen[83], V.E. Ozcan[19a], N. Ozturk[8], K. Pachal[119], A. Pacheco Pages[12], C. Padilla Aranda[12], M. Pagáčová[48], S. Pagan Griso[15], E. Paganis[140], C. Pahl[100], F. Paige[25], P. Pais[85], K. Pajchel[118], G. Palacino[160b], S. Palestini[30], D. Pallin[34], A. Palma[125a,125b], J.D. Palmer[18], Y.B. Pan[174], E. Panagiotopoulou[10], J.G. Panduro Vazquez[76], P. Pani[106], N. Panikashvili[88], S. Panitkin[25], D. Pantea[26a], L. Paolozzi[134a,134b], Th.D. Papadopoulou[10],

JHEP06(2014)112

K. Papageorgiou[155,j], A. Paramonov[6], D. Paredes Hernandez[34], M.A. Parker[28], F. Parodi[50a,50b], J.A. Parsons[35], U. Parzefall[48], E. Pasqualucci[133a], S. Passaggio[50a], A. Passeri[135a], F. Pastore[135a,135b,*], Fr. Pastore[76], G. Pásztor[49,z], S. Pataraia[176], N.D. Patel[151], J.R. Pater[83], S. Patricelli[103a,103b], T. Pauly[30], J. Pearce[170], M. Pedersen[118], S. Pedraza Lopez[168], R. Pedro[125a,125b], S.V. Peleganchuk[108], D. Pelikan[167], H. Peng[33b], B. Penning[31], J. Penwell[60], D.V. Perepelitsa[25], E. Perez Codina[160a], M.T. Pérez García-Estañ[168], V. Perez Reale[35], L. Perini[90a,90b], H. Pernegger[30], R. Perrino[72a], R. Peschke[42], V.D. Peshekhonov[64], K. Peters[30], R.F.Y. Peters[83], B.A. Petersen[87], J. Petersen[30], T.C. Petersen[36], E. Petit[42], A. Petridis[147a,147b], C. Petridou[155], E. Petrolo[133a], F. Petrucci[135a,135b], M. Petteni[143], N.E. Pettersson[158], R. Pezoa[32b], P.W. Phillips[130], G. Piacquadio[144], E. Pianori[171], A. Picazio[49], E. Piccaro[75], M. Piccinini[20a,20b], S.M. Piec[42], R. Piegaia[27], D.T. Pignotti[110], J.E. Pilcher[31], A.D. Pilkington[77], J. Pina[125a,125b,125d], M. Pinamonti[165a,165c,aa], A. Pinder[119], J.L. Pinfold[3], A. Pingel[36], B. Pinto[125a], S. Pires[79], M. Pitt[173], C. Pizio[90a,90b], M.-A. Pleier[25], V. Pleskot[128], E. Plotnikova[64], P. Plucinski[147a,147b], S. Poddar[58a], F. Podlyski[34], R. Poettgen[82], L. Poggioli[116], D. Pohl[21], M. Pohl[49], G. Polesello[120a], A. Policicchio[37a,37b], R. Polifka[159], A. Polini[20a], C.S. Pollard[45], V. Polychronakos[25], K. Pommès[30], L. Pontecorvo[133a], B.G. Pope[89], G.A. Popeneciu[26b], D.S. Popovic[13a], A. Poppleton[30], X. Portell Bueso[12], G.E. Pospelov[100], S. Pospisil[127], K. Potamianos[15], I.N. Potrap[64], C.J. Potter[150], C.T. Potter[115], G. Poulard[30], J. Poveda[60], V. Pozdnyakov[64], R. Prabhu[77], P. Pralavorio[84], A. Pranko[15], S. Prasad[30], R. Pravahan[8], S. Prell[63], D. Price[83], J. Price[73], L.E. Price[6], D. Prieur[124], M. Primavera[72a], M. Proissl[46], K. Prokofiev[109], F. Prokoshin[32b], E. Protopapadaki[137], S. Protopopescu[25], J. Proudfoot[6], M. Przybycien[38a], H. Przysiezniak[5], E. Ptacek[115], E. Pueschel[85], D. Puldon[149], M. Purohit[25,ab], P. Puzo[116], Y. Pylypchenko[62], J. Qian[88], G. Qin[53], A. Quadt[54], D.R. Quarrie[15], W.B. Quayle[165a,165b], D. Quilty[53], A. Qureshi[160b], V. Radeka[25], V. Radescu[42], S.K. Radhakrishnan[149], P. Radloff[115], P. Rados[87], F. Ragusa[90a,90b], G. Rahal[179], S. Rajagopalan[25], M. Rammensee[30], M. Rammes[142], A.S. Randle-Conde[40], C. Rangel-Smith[79], K. Rao[164], F. Rauscher[99], T.C. Rave[48], T. Ravenscroft[53], M. Raymond[30], A.L. Read[118], D.M. Rebuzzi[120a,120b], A. Redelbach[175], G. Redlinger[25], R. Reece[138], K. Reeves[41], L. Rehnisch[16], A. Reinsch[115], H. Reisin[27], M. Relich[164], C. Rembser[30], Z.L. Ren[152], A. Renaud[116], M. Rescigno[133a], S. Resconi[90a], B. Resende[137], P. Reznicek[128], R. Rezvani[94], R. Richter[100], M. Ridel[79], P. Rieck[16], M. Rijssenbeek[149], A. Rimoldi[120a,120b], L. Rinaldi[20a], E. Ritsch[61], I. Riu[12], F. Rizatdinova[113], E. Rizvi[75], S.H. Robertson[86,i], A. Robichaud-Veronneau[119], D. Robinson[28], J.E.M. Robinson[83], A. Robson[53], C. Roda[123a,123b], L. Rodrigues[30], S. Roe[30], O. Røhne[118], S. Rolli[162], A. Romaniouk[97], M. Romano[20a,20b], G. Romeo[27], E. Romero Adam[168], N. Rompotis[139], L. Roos[79], E. Ros[168], S. Rosati[133a], K. Rosbach[49], M. Rose[76], P.L. Rosendahl[14], O. Rosenthal[142], V. Rossetti[147a,147b], E. Rossi[103a,103b], L.P. Rossi[50a], R. Rosten[139], M. Rotaru[26a], I. Roth[173], J. Rothberg[139], D. Rousseau[116], C.R. Royon[137], A. Rozanov[84], Y. Rozen[153], X. Ruan[146c], F. Rubbo[12], I. Rubinskiy[42], V.I. Rud[98], C. Rudolph[44], M.S. Rudolph[159], F. Rühr[48], A. Ruiz-Martinez[63], Z. Rurikova[48], N.A. Rusakovich[64], A. Ruschke[99], J.P. Rutherfoord[7], N. Ruthmann[48], Y.F. Ryabov[122], M. Rybar[128], G. Rybkin[116], N.C. Ryder[119], A.F. Saavedra[151], S. Sacerdoti[27], A. Saddique[3], I. Sadeh[154], H.F-W. Sadrozinski[138], R. Sadykov[64], F. Safai Tehrani[133a], H. Sakamoto[156], Y. Sakurai[172], G. Salamanna[75], A. Salamon[134a], M. Saleem[112], D. Salek[106], P.H. Sales De Bruin[139], D. Salihagic[100], A. Salnikov[144], J. Salt[168], B.M. Salvachua Ferrando[6], D. Salvatore[37a,37b], F. Salvatore[150], A. Salvucci[105], A. Salzburger[30], D. Sampsonidis[155], A. Sanchez[103a,103b], J. Sánchez[168], V. Sanchez Martinez[168], H. Sandaker[14], H.G. Sander[82], M.P. Sanders[99], M. Sandhoff[176], T. Sandoval[28], C. Sandoval[163], R. Sandstroem[100], D.P.C. Sankey[130], A. Sansoni[47], C. Santoni[34], R. Santonico[134a,134b], H. Santos[125a], I. Santoyo Castillo[150], K. Sapp[124], A. Sapronov[64], J.G. Saraiva[125a,125d], B. Sarrazin[21],

JHEP06(2014)112

G. Sartisohn[176], O. Sasaki[65], Y. Sasaki[156], I. Satsounkevitch[91], G. Sauvage[5,*], E. Sauvan[5], P. Savard[159,d], D.O. Savu[30], C. Sawyer[119], L. Sawyer[78,k], D.H. Saxon[53], J. Saxon[121], C. Sbarra[20a], A. Sbrizzi[3], T. Scanlon[30], D.A. Scannicchio[164], M. Scarcella[151], J. Schaarschmidt[173], P. Schacht[100], D. Schaefer[121], R. Schaefer[42], A. Schaelicke[46], S. Schaepe[21], S. Schaetzel[58b], U. Schäfer[82], A.C. Schaffer[116], D. Schaile[99], R.D. Schamberger[149], V. Scharf[58a], V.A. Schegelsky[122], D. Scheirich[128], M. Schernau[164], M.I. Scherzer[35], C. Schiavi[50a,50b], J. Schieck[99], C. Schillo[48], M. Schioppa[37a,37b], S. Schlenker[30], E. Schmidt[48], K. Schmieden[30], C. Schmitt[82], C. Schmitt[99], S. Schmitt[58b], B. Schneider[17], Y.J. Schnellbach[73], U. Schnoor[44], L. Schoeffel[137], A. Schoening[58b], B.D. Schoenrock[89], A.L.S. Schorlemmer[54], M. Schott[82], D. Schouten[160a], J. Schovancova[25], M. Schram[86], S. Schramm[159], M. Schreyer[175], C. Schroeder[82], N. Schuh[82], M.J. Schultens[21], H.-C. Schultz-Coulon[58a], H. Schulz[16], M. Schumacher[48], B.A. Schumm[138], Ph. Schune[137], A. Schwartzman[144], Ph. Schwegler[100], Ph. Schwemling[137], R. Schwienhorst[89], J. Schwindling[137], T. Schwindt[21], M. Schwoerer[5], F.G. Sciacca[17], E. Scifo[116], G. Sciolla[23], W.G. Scott[130], F. Scuri[123a,123b], F. Scutti[21], J. Searcy[88], G. Sedov[42], E. Sedykh[122], S.C. Seidel[104], A. Seiden[138], F. Seifert[127], J.M. Seixas[24a], G. Sekhniaidze[103a], S.J. Sekula[40], K.E. Selbach[46], D.M. Seliverstov[122,*], G. Sellers[73], N. Semprini-Cesari[20a,20b], C. Serfon[30], L. Serin[116], L. Serkin[54], T. Serre[84], R. Seuster[160a], H. Severini[112], F. Sforza[100], A. Sfyrla[30], E. Shabalina[54], M. Shamim[115], L.Y. Shan[33a], J.T. Shank[22], Q.T. Shao[87], M. Shapiro[15], P.B. Shatalov[96], K. Shaw[165a,165b], P. Sherwood[77], S. Shimizu[66], C.O. Shimmin[164], M. Shimojima[101], T. Shin[56], M. Shiyakova[64], A. Shmeleva[95], M.J. Shochet[31], D. Short[119], S. Shrestha[63], E. Shulga[97], M.A. Shupe[7], S. Shushkevich[42], P. Sicho[126], D. Sidorov[113], A. Sidoti[133a], F. Siegert[44], Dj. Sijacki[13a], O. Silbert[173], J. Silva[125a,125d], Y. Silver[154], D. Silverstein[144], S.B. Silverstein[147a], V. Simak[127], O. Simard[5], Lj. Simic[13a], S. Simion[116], E. Simioni[82], B. Simmons[77], R. Simoniello[90a,90b], M. Simonyan[36], P. Sinervo[159], N.B. Sinev[115], V. Sipica[142], G. Siragusa[175], A. Sircar[78], A.N. Sisakyan[64,*], S.Yu. Sivoklokov[98], J. Sjölin[147a,147b], T.B. Sjursen[14], L.A. Skinnari[15], H.P. Skottowe[57], K.Yu. Skovpen[108], P. Skubic[112], M. Slater[18], T. Slavicek[127], K. Sliwa[162], V. Smakhtin[173], B.H. Smart[46], L. Smestad[118], S.Yu. Smirnov[97], Y. Smirnov[97], L.N. Smirnova[98,ac], O. Smirnova[80], K.M. Smith[53], M. Smizanska[71], K. Smolek[127], A.A. Snesarev[95], G. Snidero[75], J. Snow[112], S. Snyder[25], R. Sobie[170,i], F. Socher[44], J. Sodomka[127], A. Soffer[154], D.A. Soh[152,r], C.A. Solans[30], M. Solar[127], J. Solc[127], E.Yu. Soldatov[97], U. Soldevila[168], E. Solfaroli Camillocci[133a,133b], A.A. Solodkov[129], O.V. Solovyanov[129], V. Solovyev[122], P. Sommer[48], H.Y. Song[33b], N. Soni[1], A. Sood[15], A. Sopczak[127], V. Sopko[127], B. Sopko[127], V. Sorin[12], M. Sosebee[8], R. Soualah[165a,165c], P. Soueid[94], A.M. Soukharev[108], D. South[42], S. Spagnolo[72a,72b], F. Spanò[76], W.R. Spearman[57], R. Spighi[20a], G. Spigo[30], M. Spousta[128], T. Spreitzer[159], B. Spurlock[8], R.D. St. Denis[53], S. Staerz[44], J. Stahlman[121], R. Stamen[58a], E. Stanecka[39], R.W. Stanek[6], C. Stanescu[135a], M. Stanescu-Bellu[42], M.M. Stanitzki[42], S. Stapnes[118], E.A. Starchenko[129], J. Stark[55], P. Staroba[126], P. Starovoitov[42], R. Staszewski[39], P. Stavina[145a,*], G. Steele[53], P. Steinberg[25], I. Stekl[127], B. Stelzer[143], H.J. Stelzer[30], O. Stelzer-Chilton[160a], H. Stenzel[52], S. Stern[100], G.A. Stewart[53], J.A. Stillings[21], M.C. Stockton[86], M. Stoebe[86], K. Stoerig[48], G. Stoicea[26a], P. Stolte[54], S. Stonjek[100], A.R. Stradling[8], A. Straessner[44], J. Strandberg[148], S. Strandberg[147a,147b], A. Strandlie[118], E. Strauss[144], M. Strauss[112], P. Strizenec[145b], R. Ströhmer[175], D.M. Strom[115], R. Stroynowski[40], S.A. Stucci[17], B. Stugu[14], N.A. Styles[42], D. Su[144], J. Su[124], HS. Subramania[3], R. Subramaniam[78], A. Succurro[12], Y. Sugaya[117], C. Suhr[107], M. Suk[127], V.V. Sulin[95], S. Sultansoy[4c], T. Sumida[67], X. Sun[33a], J.E. Sundermann[48], K. Suruliz[140], G. Susinno[37a,37b], M.R. Sutton[150], Y. Suzuki[65], M. Svatos[126], S. Swedish[169], M. Swiatlowski[144], I. Sykora[145a], T. Sykora[128], D. Ta[89], K. Tackmann[42], J. Taenzer[159], A. Taffard[164], R. Tafirout[160a], N. Taiblum[154], Y. Takahashi[102], H. Takai[25], R. Takashima[68], H. Takeda[66], T. Takeshita[141], Y. Takubo[65], M. Talby[84],

JHEP06(2014)112

A.A. Talyshev[108,f], J.Y.C. Tam[175], M.C. Tamsett[78,ad], K.G. Tan[87], J. Tanaka[156], R. Tanaka[116], S. Tanaka[132], S. Tanaka[65], A.J. Tanasijczuk[143], K. Tani[66], N. Tannoury[84], S. Tapprogge[82], S. Tarem[153], F. Tarrade[29], G.F. Tartarelli[90a], P. Tas[128], M. Tasevsky[126], T. Tashiro[67], E. Tassi[37a,37b], A. Tavares Delgado[125a,125b], Y. Tayalati[136d], C. Taylor[77], F.E. Taylor[93], G.N. Taylor[87], W. Taylor[160b], F.A. Teischinger[30], M. Teixeira Dias Castanheira[75], P. Teixeira-Dias[76], K.K. Temming[48], H. Ten Kate[30], P.K. Teng[152], S. Terada[65], K. Terashi[156], J. Terron[81], S. Terzo[100], M. Testa[47], R.J. Teuscher[159,i], J. Therhaag[21], T. Theveneaux-Pelzer[34], S. Thoma[48], J.P. Thomas[18], J. Thomas-Wilsker[76], E.N. Thompson[35], P.D. Thompson[18], P.D. Thompson[159], A.S. Thompson[53], L.A. Thomsen[36], E. Thomson[121], M. Thomson[28], W.M. Thong[87], R.P. Thun[88,*], F. Tian[35], M.J. Tibbetts[15], V.O. Tikhomirov[95,ae], Yu.A. Tikhonov[108,f], S. Timoshenko[97], E. Tiouchichine[84], P. Tipton[177], S. Tisserant[84], T. Todorov[5], S. Todorova-Nova[128], B. Toggerson[164], J. Tojo[69], S. Tokár[145a], K. Tokushuku[65], K. Tollefson[89], L. Tomlinson[83], M. Tomoto[102], L. Tompkins[31], K. Toms[104], N.D. Topilin[64], E. Torrence[115], H. Torres[143], E. Torró Pastor[168], J. Toth[84,z], F. Touchard[84], D.R. Tovey[140], H.L. Tran[116], T. Trefzger[175], L. Tremblet[30], A. Tricoli[30], I.M. Trigger[160a], S. Trincaz-Duvoid[79], M.F. Tripiana[70], N. Triplett[25], W. Trischuk[159], B. Trocmé[55], C. Troncon[90a], M. Trottier-McDonald[143], M. Trovatelli[135a,135b], P. True[89], M. Trzebinski[39], A. Trzupek[39], C. Tsarouchas[30], J.C-L. Tseng[119], P.V. Tsiareshka[91], D. Tsionou[137], G. Tsipolitis[10], N. Tsirintanis[9], S. Tsiskaridze[12], V. Tsiskaridze[48], E.G. Tskhadadze[51a], I.I. Tsukerman[96], V. Tsulaia[15], S. Tsuno[65], D. Tsybychev[149], A. Tua[140], A. Tudorache[26a], V. Tudorache[26a], A.N. Tuna[121], S.A. Tupputi[20a,20b], S. Turchikhin[98,ac], D. Turecek[127], I. Turk Cakir[4d], R. Turra[90a,90b], P.M. Tuts[35], A. Tykhonov[74], M. Tylmad[147a,147b], M. Tyndel[130], K. Uchida[21], I. Ueda[156], R. Ueno[29], M. Ughetto[84], M. Ugland[14], M. Uhlenbrock[21], F. Ukegawa[161], G. Unal[30], A. Undrus[25], G. Unel[164], F.C. Ungaro[48], Y. Unno[65], D. Urbaniec[35], P. Urquijo[21], G. Usai[8], A. Usanova[61], L. Vacavant[84], V. Vacek[127], B. Vachon[86], N. Valencic[106], S. Valentinetti[20a,20b], A. Valero[168], L. Valery[34], S. Valkar[128], E. Valladolid Gallego[168], S. Vallecorsa[49], J.A. Valls Ferrer[168], R. Van Berg[121], P.C. Van Der Deijl[106], R. van der Geer[106], H. van der Graaf[106], R. Van Der Leeuw[106], D. van der Ster[30], N. van Eldik[30], P. van Gemmeren[6], J. Van Nieuwkoop[143], I. van Vulpen[106], M.C. van Woerden[30], M. Vanadia[133a,133b], W. Vandelli[30], R. Vanguri[121], A. Vaniachine[6], P. Vankov[42], F. Vannucci[79], G. Vardanyan[178], R. Vari[133a], E.W. Varnes[7], T. Varol[85], D. Varouchas[79], A. Vartapetian[8], K.E. Varvell[151], V.I. Vassilakopoulos[56], F. Vazeille[34], T. Vazquez Schroeder[54], J. Veatch[7], F. Veloso[125a,125c], S. Veneziano[133a], A. Ventura[72a,72b], D. Ventura[85], M. Venturi[48], N. Venturi[159], A. Venturini[23], V. Vercesi[120a], M. Verducci[139], W. Verkerke[106], J.C. Vermeulen[106], A. Vest[44], M.C. Vetterli[143,d], O. Viazlo[80], I. Vichou[166], T. Vickey[146c,af], O.E. Vickey Boeriu[146c], G.H.A. Viehhauser[119], S. Viel[169], R. Vigne[30], M. Villa[20a,20b], M. Villaplana Perez[168], E. Vilucchi[47], M.G. Vincter[29], V.B. Vinogradov[64], J. Virzi[15], O. Vitells[173], I. Vivarelli[150], F. Vives Vaque[3], S. Vlachos[10], D. Vladoiu[99], M. Vlasak[127], A. Vogel[21], P. Vokac[127], G. Volpi[47], M. Volpi[87], H. von der Schmitt[100], H. von Radziewski[48], E. von Toerne[21], V. Vorobel[128], K. Vorobev[97], M. Vos[168], R. Voss[30], J.H. Vossebeld[73], N. Vranjes[137], M. Vranjes Milosavljevic[106], V. Vrba[126], M. Vreeswijk[106], T. Vu Anh[48], R. Vuillermet[30], I. Vukotic[31], Z. Vykydal[127], W. Wagner[176], P. Wagner[21], S. Wahrmund[44], J. Wakabayashi[102], J. Walder[71], R. Walker[99], W. Walkowiak[142], R. Wall[177], P. Waller[73], B. Walsh[177], C. Wang[152], C. Wang[45], F. Wang[174], H. Wang[15], H. Wang[40], J. Wang[42], J. Wang[33a], K. Wang[86], R. Wang[104], S.M. Wang[152], T. Wang[21], X. Wang[177], A. Warburton[86], C.P. Ward[28], D.R. Wardrope[77], M. Warsinsky[48], A. Washbrook[46], C. Wasicki[42], I. Watanabe[66], P.M. Watkins[18], A.T. Watson[18], I.J. Watson[151], M.F. Watson[18], G. Watts[139], S. Watts[83], B.M. Waugh[77], S. Webb[83], M.S. Weber[17], S.W. Weber[175], J.S. Webster[31], A.R. Weidberg[119], P. Weigell[100], B. Weinert[60], J. Weingarten[54], C. Weiser[48],

JHEP06(2014)112

H. Weits[106], P.S. Wells[30], T. Wenaus[25], D. Wendland[16], Z. Weng[152,r], T. Wengler[30], S. Wenig[30], N. Wermes[21], M. Werner[48], P. Werner[30], M. Wessels[58a], J. Wetter[162], K. Whalen[29], A. White[8], M.J. White[1], R. White[32b], S. White[123a,123b], D. Whiteson[164], D. Wicke[176], F.J. Wickens[130], W. Wiedenmann[174], M. Wielers[130], P. Wienemann[21], C. Wiglesworth[36], L.A.M. Wiik-Fuchs[21], P.A. Wijeratne[77], A. Wildauer[100], M.A. Wildt[42,ag], H.G. Wilkens[30], J.Z. Will[99], H.H. Williams[121], S. Williams[28], C. Willis[89], S. Willocq[85], J.A. Wilson[18], A. Wilson[88], I. Wingerter-Seez[5], S. Winkelmann[48], F. Winklmeier[115], M. Wittgen[144], T. Wittig[43], J. Wittkowski[99], S.J. Wollstadt[82], M.W. Wolter[39], H. Wolters[125a,125c], B.K. Wosiek[39], J. Wotschack[30], M.J. Woudstra[83], K.W. Wozniak[39], M. Wright[53], M. Wu[55], S.L. Wu[174], X. Wu[49], Y. Wu[88], E. Wulf[35], T.R. Wyatt[83], B.M. Wynne[46], S. Xella[36], M. Xiao[137], D. Xu[33a], L. Xu[33b,ah], B. Yabsley[151], S. Yacoob[146b,ai], M. Yamada[65], H. Yamaguchi[156], Y. Yamaguchi[156], A. Yamamoto[65], K. Yamamoto[63], S. Yamamoto[156], T. Yamamura[156], T. Yamanaka[156], K. Yamauchi[102], Y. Yamazaki[66], Z. Yan[22], H. Yang[33e], H. Yang[174], U.K. Yang[83], Y. Yang[110], S. Yanush[92], L. Yao[33a], W-M. Yao[15], Y. Yasu[65], E. Yatsenko[42], K.H. Yau Wong[21], J. Ye[40], S. Ye[25], A.L. Yen[57], E. Yildirim[42], M. Yilmaz[4b], R. Yoosoofmiya[124], K. Yorita[172], R. Yoshida[6], K. Yoshihara[156], C. Young[144], C.J.S. Young[30], S. Youssef[22], D.R. Yu[15], J. Yu[8], J.M. Yu[88], J. Yu[113], L. Yuan[66], A. Yurkewicz[107], B. Zabinski[39], R. Zaidan[62], A.M. Zaitsev[129,w], A. Zaman[149], S. Zambito[23], L. Zanello[133a,133b], D. Zanzi[100], A. Zaytsev[25], C. Zeitnitz[176], M. Zeman[127], A. Zemla[38a], K. Zengel[23], O. Zenin[129], T. Ženiš[145a], D. Zerwas[116], G. Zevi della Porta[57], D. Zhang[88], F. Zhang[174], H. Zhang[89], J. Zhang[6], L. Zhang[152], X. Zhang[33d], Z. Zhang[116], Z. Zhao[33b], A. Zhemchugov[64], J. Zhong[119], B. Zhou[88], L. Zhou[35], N. Zhou[164], C.G. Zhu[33d], H. Zhu[33a], J. Zhu[88], Y. Zhu[33b], X. Zhuang[33a], A. Zibell[99], D. Zieminska[60], N.I. Zimine[64], C. Zimmermann[82], R. Zimmermann[21], S. Zimmermann[21], S. Zimmermann[48], Z. Zinonos[54], M. Ziolkowski[142], R. Zitoun[5], G. Zobernig[174], A. Zoccoli[20a,20b], M. zur Nedden[16], G. Zurzolo[103a,103b], V. Zutshi[107] and L. Zwalinski[30].

[1] *Department of Physics, University of Adelaide, Adelaide, Australia*
[2] *Physics Department, SUNY Albany, Albany NY, United States of America*
[3] *Department of Physics, University of Alberta, Edmonton AB, Canada*
[4] [(a)] *Department of Physics, Ankara University, Ankara;* [(b)] *Department of Physics, Gazi University, Ankara;* [(c)] *Division of Physics, TOBB University of Economics and Technology, Ankara;* [(d)] *Turkish Atomic Energy Authority, Ankara, Turkey*
[5] *LAPP, CNRS/IN2P3 and Université de Savoie, Annecy-le-Vieux, France*
[6] *High Energy Physics Division, Argonne National Laboratory, Argonne IL, United States of America*
[7] *Department of Physics, University of Arizona, Tucson AZ, United States of America*
[8] *Department of Physics, The University of Texas at Arlington, Arlington TX, United States of America*
[9] *Physics Department, University of Athens, Athens, Greece*
[10] *Physics Department, National Technical University of Athens, Zografou, Greece*
[11] *Institute of Physics, Azerbaijan Academy of Sciences, Baku, Azerbaijan*
[12] *Institut de Física d'Altes Energies and Departament de Física de la Universitat Autònoma de Barcelona, Barcelona, Spain*
[13] [(a)] *Institute of Physics, University of Belgrade, Belgrade;* [(b)] *Vinca Institute of Nuclear Sciences, University of Belgrade, Belgrade, Serbia*
[14] *Department for Physics and Technology, University of Bergen, Bergen, Norway*
[15] *Physics Division, Lawrence Berkeley National Laboratory and University of California, Berkeley CA, United States of America*
[16] *Department of Physics, Humboldt University, Berlin, Germany*
[17] *Albert Einstein Center for Fundamental Physics and Laboratory for High Energy Physics, University of Bern, Bern, Switzerland*

JHEP06(2014)112

[18] School of Physics and Astronomy, University of Birmingham, Birmingham, United Kingdom
[19] [(a)] Department of Physics, Bogazici University, Istanbul; [(b)] Department of Physics, Dogus University, Istanbul; [(c)] Department of Physics Engineering, Gaziantep University, Gaziantep, Turkey
[20] [(a)] INFN Sezione di Bologna; [(b)] Dipartimento di Fisica e Astronomia, Università di Bologna, Bologna, Italy
[21] Physikalisches Institut, University of Bonn, Bonn, Germany
[22] Department of Physics, Boston University, Boston MA, United States of America
[23] Department of Physics, Brandeis University, Waltham MA, United States of America
[24] [(a)] Universidade Federal do Rio De Janeiro COPPE/EE/IF, Rio de Janeiro; [(b)] Federal University of Juiz de Fora (UFJF), Juiz de Fora; [(c)] Federal University of Sao Joao del Rei (UFSJ), Sao Joao del Rei; [(d)] Instituto de Fisica, Universidade de Sao Paulo, Sao Paulo, Brazil
[25] Physics Department, Brookhaven National Laboratory, Upton NY, United States of America
[26] [(a)] National Institute of Physics and Nuclear Engineering, Bucharest; [(b)] National Institute for Research and Development of Isotopic and Molecular Technologies, Physics Department, Cluj Napoca; [(c)] University Politehnica Bucharest, Bucharest; [(d)] West University in Timisoara, Timisoara, Romania
[27] Departamento de Física, Universidad de Buenos Aires, Buenos Aires, Argentina
[28] Cavendish Laboratory, University of Cambridge, Cambridge, United Kingdom
[29] Department of Physics, Carleton University, Ottawa ON, Canada
[30] CERN, Geneva, Switzerland
[31] Enrico Fermi Institute, University of Chicago, Chicago IL, United States of America
[32] [(a)] Departamento de Física, Pontificia Universidad Católica de Chile, Santiago; [(b)] Departamento de Física, Universidad Técnica Federico Santa María, Valparaíso, Chile
[33] [(a)] Institute of High Energy Physics, Chinese Academy of Sciences, Beijing; [(b)] Department of Modern Physics, University of Science and Technology of China, Anhui; [(c)] Department of Physics, Nanjing University, Jiangsu; [(d)] School of Physics, Shandong University, Shandong; [(e)] Physics Department, Shanghai Jiao Tong University, Shanghai, China
[34] Laboratoire de Physique Corpusculaire, Clermont Université and Université Blaise Pascal and CNRS/IN2P3, Clermont-Ferrand, France
[35] Nevis Laboratory, Columbia University, Irvington NY, United States of America
[36] Niels Bohr Institute, University of Copenhagen, Kobenhavn, Denmark
[37] [(a)] INFN Gruppo Collegato di Cosenza, Laboratori Nazionali di Frascati; [(b)] Dipartimento di Fisica, Università della Calabria, Rende, Italy
[38] [(a)] AGH University of Science and Technology, Faculty of Physics and Applied Computer Science, Krakow; [(b)] Marian Smoluchowski Institute of Physics, Jagiellonian University, Krakow, Poland
[39] The Henryk Niewodniczanski Institute of Nuclear Physics, Polish Academy of Sciences, Krakow, Poland
[40] Physics Department, Southern Methodist University, Dallas TX, United States of America
[41] Physics Department, University of Texas at Dallas, Richardson TX, United States of America
[42] DESY, Hamburg and Zeuthen, Germany
[43] Institut für Experimentelle Physik IV, Technische Universität Dortmund, Dortmund, Germany
[44] Institut für Kern- und Teilchenphysik, Technische Universität Dresden, Dresden, Germany
[45] Department of Physics, Duke University, Durham NC, United States of America
[46] SUPA - School of Physics and Astronomy, University of Edinburgh, Edinburgh, United Kingdom
[47] INFN Laboratori Nazionali di Frascati, Frascati, Italy
[48] Fakultät für Mathematik und Physik, Albert-Ludwigs-Universität, Freiburg, Germany
[49] Section de Physique, Université de Genève, Geneva, Switzerland
[50] [(a)] INFN Sezione di Genova; [(b)] Dipartimento di Fisica, Università di Genova, Genova, Italy
[51] [(a)] E. Andronikashvili Institute of Physics, Iv. Javakhishvili Tbilisi State University, Tbilisi; [(b)] High Energy Physics Institute, Tbilisi State University, Tbilisi, Georgia
[52] II Physikalisches Institut, Justus-Liebig-Universität Giessen, Giessen, Germany

JHEP06(2014)112

[53] SUPA - School of Physics and Astronomy, University of Glasgow, Glasgow, United Kingdom
[54] II Physikalisches Institut, Georg-August-Universität, Göttingen, Germany
[55] Laboratoire de Physique Subatomique et de Cosmologie, Université Joseph Fourier and CNRS/IN2P3 and Institut National Polytechnique de Grenoble, Grenoble, France
[56] Department of Physics, Hampton University, Hampton VA, United States of America
[57] Laboratory for Particle Physics and Cosmology, Harvard University, Cambridge MA, United States of America
[58] [(a)] Kirchhoff-Institut für Physik, Ruprecht-Karls-Universität Heidelberg, Heidelberg; [(b)] Physikalisches Institut, Ruprecht-Karls-Universität Heidelberg, Heidelberg; [(c)] ZITI Institut für technische Informatik, Ruprecht-Karls-Universität Heidelberg, Mannheim, Germany
[59] Faculty of Applied Information Science, Hiroshima Institute of Technology, Hiroshima, Japan
[60] Department of Physics, Indiana University, Bloomington IN, United States of America
[61] Institut für Astro- und Teilchenphysik, Leopold-Franzens-Universität, Innsbruck, Austria
[62] University of Iowa, Iowa City IA, United States of America
[63] Department of Physics and Astronomy, Iowa State University, Ames IA, United States of America
[64] Joint Institute for Nuclear Research, JINR Dubna, Dubna, Russia
[65] KEK, High Energy Accelerator Research Organization, Tsukuba, Japan
[66] Graduate School of Science, Kobe University, Kobe, Japan
[67] Faculty of Science, Kyoto University, Kyoto, Japan
[68] Kyoto University of Education, Kyoto, Japan
[69] Department of Physics, Kyushu University, Fukuoka, Japan
[70] Instituto de Física La Plata, Universidad Nacional de La Plata and CONICET, La Plata, Argentina
[71] Physics Department, Lancaster University, Lancaster, United Kingdom
[72] [(a)] INFN Sezione di Lecce; [(b)] Dipartimento di Matematica e Fisica, Università del Salento, Lecce, Italy
[73] Oliver Lodge Laboratory, University of Liverpool, Liverpool, United Kingdom
[74] Department of Physics, Jožef Stefan Institute and University of Ljubljana, Ljubljana, Slovenia
[75] School of Physics and Astronomy, Queen Mary University of London, London, United Kingdom
[76] Department of Physics, Royal Holloway University of London, Surrey, United Kingdom
[77] Department of Physics and Astronomy, University College London, London, United Kingdom
[78] Louisiana Tech University, Ruston LA, United States of America
[79] Laboratoire de Physique Nucléaire et de Hautes Energies, UPMC and Université Paris-Diderot and CNRS/IN2P3, Paris, France
[80] Fysiska institutionen, Lunds universitet, Lund, Sweden
[81] Departamento de Fisica Teorica C-15, Universidad Autonoma de Madrid, Madrid, Spain
[82] Institut für Physik, Universität Mainz, Mainz, Germany
[83] School of Physics and Astronomy, University of Manchester, Manchester, United Kingdom
[84] CPPM, Aix-Marseille Université and CNRS/IN2P3, Marseille, France
[85] Department of Physics, University of Massachusetts, Amherst MA, United States of America
[86] Department of Physics, McGill University, Montreal QC, Canada
[87] School of Physics, University of Melbourne, Victoria, Australia
[88] Department of Physics, The University of Michigan, Ann Arbor MI, United States of America
[89] Department of Physics and Astronomy, Michigan State University, East Lansing MI, United States of America
[90] [(a)] INFN Sezione di Milano; [(b)] Dipartimento di Fisica, Università di Milano, Milano, Italy
[91] B.I. Stepanov Institute of Physics, National Academy of Sciences of Belarus, Minsk, Republic of Belarus
[92] National Scientific and Educational Centre for Particle and High Energy Physics, Minsk, Republic of Belarus
[93] Department of Physics, Massachusetts Institute of Technology, Cambridge MA, United States of America
[94] Group of Particle Physics, University of Montreal, Montreal QC, Canada

JHEP06(2014)112

[95] P.N. Lebedev Institute of Physics, Academy of Sciences, Moscow, Russia
[96] Institute for Theoretical and Experimental Physics (ITEP), Moscow, Russia
[97] Moscow Engineering and Physics Institute (MEPhI), Moscow, Russia
[98] D.V.Skobeltsyn Institute of Nuclear Physics, M.V.Lomonosov Moscow State University, Moscow, Russia
[99] Fakultät für Physik, Ludwig-Maximilians-Universität München, München, Germany
[100] Max-Planck-Institut für Physik (Werner-Heisenberg-Institut), München, Germany
[101] Nagasaki Institute of Applied Science, Nagasaki, Japan
[102] Graduate School of Science and Kobayashi-Maskawa Institute, Nagoya University, Nagoya, Japan
[103] [(a)] INFN Sezione di Napoli; [(b)] Dipartimento di Fisica, Università di Napoli, Napoli, Italy
[104] Department of Physics and Astronomy, University of New Mexico, Albuquerque NM, United States of America
[105] Institute for Mathematics, Astrophysics and Particle Physics, Radboud University Nijmegen/Nikhef, Nijmegen, Netherlands
[106] Nikhef National Institute for Subatomic Physics and University of Amsterdam, Amsterdam, Netherlands
[107] Department of Physics, Northern Illinois University, DeKalb IL, United States of America
[108] Budker Institute of Nuclear Physics, SB RAS, Novosibirsk, Russia
[109] Department of Physics, New York University, New York NY, United States of America
[110] Ohio State University, Columbus OH, United States of America
[111] Faculty of Science, Okayama University, Okayama, Japan
[112] Homer L. Dodge Department of Physics and Astronomy, University of Oklahoma, Norman OK, United States of America
[113] Department of Physics, Oklahoma State University, Stillwater OK, United States of America
[114] Palacký University, RCPTM, Olomouc, Czech Republic
[115] Center for High Energy Physics, University of Oregon, Eugene OR, United States of America
[116] LAL, Université Paris-Sud and CNRS/IN2P3, Orsay, France
[117] Graduate School of Science, Osaka University, Osaka, Japan
[118] Department of Physics, University of Oslo, Oslo, Norway
[119] Department of Physics, Oxford University, Oxford, United Kingdom
[120] [(a)] INFN Sezione di Pavia; [(b)] Dipartimento di Fisica, Università di Pavia, Pavia, Italy
[121] Department of Physics, University of Pennsylvania, Philadelphia PA, United States of America
[122] Petersburg Nuclear Physics Institute, Gatchina, Russia
[123] [(a)] INFN Sezione di Pisa; [(b)] Dipartimento di Fisica E. Fermi, Università di Pisa, Pisa, Italy
[124] Department of Physics and Astronomy, University of Pittsburgh, Pittsburgh PA, United States of America
[125] [(a)] Laboratorio de Instrumentacao e Fisica Experimental de Particulas - LIP, Lisboa; [(b)] Faculdade de Ciências, Universidade de Lisboa, Lisboa; [(c)] Department of Physics, University of Coimbra, Coimbra; [(d)] Centro de Física Nuclear da Universidade de Lisboa, Lisboa; [(e)] Departamento de Fisica, Universidade do Minho, Braga; [(f)] Departamento de Fisica Teorica y del Cosmos and CAFPE, Universidad de Granada, Granada (Spain); [(g)] Dep Fisica and CEFITEC of Faculdade de Ciencias e Tecnologia, Universidade Nova de Lisboa, Caparica, Portugal
[126] Institute of Physics, Academy of Sciences of the Czech Republic, Praha, Czech Republic
[127] Czech Technical University in Prague, Praha, Czech Republic
[128] Faculty of Mathematics and Physics, Charles University in Prague, Praha, Czech Republic
[129] State Research Center Institute for High Energy Physics, Protvino, Russia
[130] Particle Physics Department, Rutherford Appleton Laboratory, Didcot, United Kingdom
[131] Physics Department, University of Regina, Regina SK, Canada
[132] Ritsumeikan University, Kusatsu, Shiga, Japan
[133] [(a)] INFN Sezione di Roma; [(b)] Dipartimento di Fisica, Sapienza Università di Roma, Roma, Italy
[134] [(a)] INFN Sezione di Roma Tor Vergata; [(b)] Dipartimento di Fisica, Università di Roma Tor Vergata, Roma, Italy

JHEP06(2014)112

[135] [(a)] INFN Sezione di Roma Tre; [(b)] Dipartimento di Matematica e Fisica, Università Roma Tre, Roma, Italy
[136] [(a)] Faculté des Sciences Ain Chock, Réseau Universitaire de Physique des Hautes Energies - Université Hassan II, Casablanca; [(b)] Centre National de l'Energie des Sciences Techniques Nucleaires, Rabat; [(c)] Faculté des Sciences Semlalia, Université Cadi Ayyad, LPHEA-Marrakech; [(d)] Faculté des Sciences, Université Mohamed Premier and LPTPM, Oujda; [(e)] Faculté des sciences, Université Mohammed V-Agdal, Rabat, Morocco
[137] DSM/IRFU (Institut de Recherches sur les Lois Fondamentales de l'Univers), CEA Saclay (Commissariat à l'Energie Atomique et aux Energies Alternatives), Gif-sur-Yvette, France
[138] Santa Cruz Institute for Particle Physics, University of California Santa Cruz, Santa Cruz CA, United States of America
[139] Department of Physics, University of Washington, Seattle WA, United States of America
[140] Department of Physics and Astronomy, University of Sheffield, Sheffield, United Kingdom
[141] Department of Physics, Shinshu University, Nagano, Japan
[142] Fachbereich Physik, Universität Siegen, Siegen, Germany
[143] Department of Physics, Simon Fraser University, Burnaby BC, Canada
[144] SLAC National Accelerator Laboratory, Stanford CA, United States of America
[145] [(a)] Faculty of Mathematics, Physics & Informatics, Comenius University, Bratislava; [(b)] Department of Subnuclear Physics, Institute of Experimental Physics of the Slovak Academy of Sciences, Kosice, Slovak Republic
[146] [(a)] Department of Physics, University of Cape Town, Cape Town; [(b)] Department of Physics, University of Johannesburg, Johannesburg; [(c)] School of Physics, University of the Witwatersrand, Johannesburg, South Africa
[147] [(a)] Department of Physics, Stockholm University; [(b)] The Oskar Klein Centre, Stockholm, Sweden
[148] Physics Department, Royal Institute of Technology, Stockholm, Sweden
[149] Departments of Physics & Astronomy and Chemistry, Stony Brook University, Stony Brook NY, United States of America
[150] Department of Physics and Astronomy, University of Sussex, Brighton, United Kingdom
[151] School of Physics, University of Sydney, Sydney, Australia
[152] Institute of Physics, Academia Sinica, Taipei, Taiwan
[153] Department of Physics, Technion: Israel Institute of Technology, Haifa, Israel
[154] Raymond and Beverly Sackler School of Physics and Astronomy, Tel Aviv University, Tel Aviv, Israel
[155] Department of Physics, Aristotle University of Thessaloniki, Thessaloniki, Greece
[156] International Center for Elementary Particle Physics and Department of Physics, The University of Tokyo, Tokyo, Japan
[157] Graduate School of Science and Technology, Tokyo Metropolitan University, Tokyo, Japan
[158] Department of Physics, Tokyo Institute of Technology, Tokyo, Japan
[159] Department of Physics, University of Toronto, Toronto ON, Canada
[160] [(a)] TRIUMF, Vancouver BC; [(b)] Department of Physics and Astronomy, York University, Toronto ON, Canada
[161] Faculty of Pure and Applied Sciences, University of Tsukuba, Tsukuba, Japan
[162] Department of Physics and Astronomy, Tufts University, Medford MA, United States of America
[163] Centro de Investigaciones, Universidad Antonio Narino, Bogota, Colombia
[164] Department of Physics and Astronomy, University of California Irvine, Irvine CA, United States of America
[165] [(a)] INFN Gruppo Collegato di Udine, Sezione di Trieste, Udine; [(b)] ICTP, Trieste; [(c)] Dipartimento di Chimica, Fisica e Ambiente, Università di Udine, Udine, Italy
[166] Department of Physics, University of Illinois, Urbana IL, United States of America
[167] Department of Physics and Astronomy, University of Uppsala, Uppsala, Sweden
[168] Instituto de Física Corpuscular (IFIC) and Departamento de Física Atómica, Molecular y Nuclear and Departamento de Ingeniería Electrónica and Instituto de Microelectrónica de Barcelona

JHEP06(2014)112

(IMB-CNM), University of Valencia and CSIC, Valencia, Spain
[169] Department of Physics, University of British Columbia, Vancouver BC, Canada
[170] Department of Physics and Astronomy, University of Victoria, Victoria BC, Canada
[171] Department of Physics, University of Warwick, Coventry, United Kingdom
[172] Waseda University, Tokyo, Japan
[173] Department of Particle Physics, The Weizmann Institute of Science, Rehovot, Israel
[174] Department of Physics, University of Wisconsin, Madison WI, United States of America
[175] Fakultät für Physik und Astronomie, Julius-Maximilians-Universität, Würzburg, Germany
[176] Fachbereich C Physik, Bergische Universität Wuppertal, Wuppertal, Germany
[177] Department of Physics, Yale University, New Haven CT, United States of America
[178] Yerevan Physics Institute, Yerevan, Armenia
[179] Centre de Calcul de l'Institut National de Physique Nucléaire et de Physique des Particules (IN2P3), Villeurbanne, France
[a] Also at Department of Physics, King's College London, London, United Kingdom
[b] Also at Institute of Physics, Azerbaijan Academy of Sciences, Baku, Azerbaijan
[c] Also at Particle Physics Department, Rutherford Appleton Laboratory, Didcot, United Kingdom
[d] Also at TRIUMF, Vancouver BC, Canada
[e] Also at Department of Physics, California State University, Fresno CA, United States of America
[f] Also at Novosibirsk State University, Novosibirsk, Russia
[g] Also at CPPM, Aix-Marseille Université and CNRS/IN2P3, Marseille, France
[h] Also at Università di Napoli Parthenope, Napoli, Italy
[i] Also at Institute of Particle Physics (IPP), Canada
[j] Also at Department of Financial and Management Engineering, University of the Aegean, Chios, Greece
[k] Also at Louisiana Tech University, Ruston LA, United States of America
[l] Also at Institucio Catalana de Recerca i Estudis Avancats, ICREA, Barcelona, Spain
[m] Also at CERN, Geneva, Switzerland
[n] Also at Ochadai Academic Production, Ochanomizu University, Tokyo, Japan
[o] Also at Manhattan College, New York NY, United States of America
[p] Also at Institute of Physics, Academia Sinica, Taipei, Taiwan
[q] Also at Department of Physics, Nanjing University, Jiangsu, China
[r] Also at School of Physics and Engineering, Sun Yat-sen University, Guangzhou, China
[s] Also at Academia Sinica Grid Computing, Institute of Physics, Academia Sinica, Taipei, Taiwan
[t] Also at Laboratoire de Physique Nucléaire et de Hautes Energies, UPMC and Université Paris-Diderot and CNRS/IN2P3, Paris, France
[u] Also at School of Physical Sciences, National Institute of Science Education and Research, Bhubaneswar, India
[v] Also at Dipartimento di Fisica, Sapienza Università di Roma, Roma, Italy
[w] Also at Moscow Institute of Physics and Technology State University, Dolgoprudny, Russia
[x] Also at section de Physique, Université de Genève, Geneva, Switzerland
[y] Also at Department of Physics, The University of Texas at Austin, Austin TX, United States of America
[z] Also at Institute for Particle and Nuclear Physics, Wigner Research Centre for Physics, Budapest, Hungary
[aa] Also at International School for Advanced Studies (SISSA), Trieste, Italy
[ab] Also at Department of Physics and Astronomy, University of South Carolina, Columbia SC, United States of America
[ac] Also at Faculty of Physics, M.V.Lomonosov Moscow State University, Moscow, Russia
[ad] Also at Physics Department, Brookhaven National Laboratory, Upton NY, United States of America
[ae] Also at Moscow Engineering and Physics Institute (MEPhI), Moscow, Russia
[af] Also at Department of Physics, Oxford University, Oxford, United Kingdom
[ag] Also at Institut für Experimentalphysik, Universität Hamburg, Hamburg, Germany

JHEP06(2014)112

[ah] *Also at Department of Physics, The University of Michigan, Ann Arbor MI, United States of America*
[ai] *Also at Discipline of Physics, University of KwaZulu-Natal, Durban, South Africa*
[*] *Deceased*

JHEP06(2014)112